A delayed-choice quantum eraser experiment with an IBM quantum computer

By Jose C. Moreno

The history of qubit q[0] was interpreted by means of two different entanglements using q[1], q[2], q[3], q[4]: on the z-basis, one entanglement was $|E1> \propto (\ |0>_0 |1>_1 |0>_2 |0>_3 |0>_0 + e^{i\varphi} |1>_0 |0>_1 |0>_2 |0>_3 |0>_0$. The other entanglement, on the z and x basis, was $|E2> \propto d(\varphi)|0>_0 |0>_1 |1>_2 |+>_3 |1>_4 + f(\varphi) |1>_0 |0>_1 |1>_2 |->_3 |1>_4 + g(\varphi) |0>_0 |0>_1 |1>_2 |->_3 |0>_4 + h(\varphi)|1>_0 |0>_1 |1>_2 |+>_3 |0>_4$; |E2> allowed to interpret the probability of q[0] to be $\propto |d(\varphi)|^2$, $|f(\varphi)|^2$, $|g(\varphi)|^2$, or $|h(\varphi)|^2$ in relation to the measurements of other qubits; each of those probabilities had either the form $\propto \cos^2(\varphi/2)$ or $\propto \sin^2(\varphi/2)$; by associating those probabilities with q[0], the history of q[0] could be interpreted to be either $A_0(\varphi)|0>_0 + B_0(\varphi)|0>$ or $C_0(\varphi)|1>_0 + D_0(\varphi)|1>$, contrasting the pattern obtained when |E1> happened; no interference pattern was detected without the measurements of q[0] when |E2> happened. In this way, neither the gates on q[0] nor |E1> created an interference pattern; the interference pattern was the result of |E2> and could be attributed to q[0] when joint measurements with the other qubits were performed. Measurements on q[0] were performed first, which were interpreted as "erasing" the history that q[0] would have had before it was measured with the other qubits in |E2>. Results obtained with the present experiment, and its analysis, offered a new interpretation to Schully's Delayed-Choice Quantum eraser experiment.

INTRODUCTION

The purpose of a delayed-choice experiment is to demonstrate instrumentally how measurements in the present, on a quantum system, allow to interpret, in more than one way, the history of the system. It was Wheeler that said, "...the photon that we are going to register tonight from that four billion year old quasar cannot be said to have existence...not until we have fixed arrangements at our telescope do we register...as having passed to the left (or right)..or by both routes…"[1] to illustrate that the past of quantum systems are not absolutely defined in any particular way before a measurement, but contrary to Bohr [3], Wheeler's interpretation suggested that was possible to describe the history of the system AFTER measurements, as if the present measurements can influence the past of the system. From a theoretical perspective, given a superposition $\psi(r)=\psi_A(r_1)+\psi_B(r_2)$, where $\psi_A(r_1)$ and $\psi_B(r_2)$ are the wave functions corresponding a quantum that is potentially moving through two separate paths r_1 and r_2, the probability is $|\psi_A(r_1)+\psi_B(r_2)|^2$ when the "which path information" is unknown, but either $|\psi_A(r_1)|^2$ or $|\psi_B(r_1)|^2$ when the path followed by the quantum is known [4]; using 3 different projectors P_{AB} , P_A , P_B such that $P_{AB}\psi(r)=\psi_A(r_1)+\psi_B(r_2)$, $P_A\psi(r)=\psi_A(r_1)$, and $P_B\psi(r)=\psi_B(r_2)$, corresponding to probabilities $|\psi_A(r_1)+\psi_B(r_2)|^2$, $|\psi_A(r_1)|^2$, $|\psi_B(r_2)|^2$ respectively, it is possible to interpret the history of the quantum in an initially prepared state $\psi(r)$, at a time $t^{present}$, as $\psi_A(r_1)+\psi_B(r_2)$, $\psi_A(r_1)$, or $\psi_B(r_2)$ when any of the operators P_{AB} , P_A , P_B is used to project $\psi(r)$ at any time $t^{present}$. In this way, if information from both paths r_1 and r_2 are allowed to reach a detecting screen and obtain an interference pattern from $|P_{AB}\psi(r)|^2$, it may be said that the quantum followed both paths; if only $|P_A\psi(r_1)|^2$ or $|P_B\psi(r_2)|^2$ were measured at the same screen, then the quantum went through either paths r_1 or r_2. It is possible to decide the interpretation of the history of the quantum based on the projector and measurements thereafter.
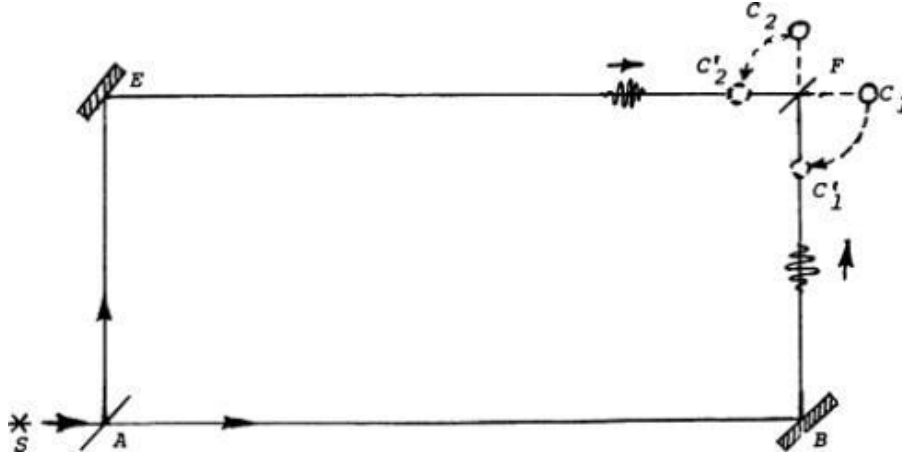
Figure 1. Schematic representation of a delayed-choice wheeler experiment; photons detected near C_2 and C_1 exhibit different probability patterns depending on the orientation of F. (Picture from "The Undivided Universe" pg.129 [2])

Wheeler's thought experiment has been demonstrated with a variety of experimental setups [6],[7]; a typical schematic illustration of an experiment is shown on fig. 1; the results from those experiments have shown that is possible to decide whether a system shows an interference pattern or not, and establish the history of the quantum system after making those measurements, as suggested by Wheeler.

However, a conceptual extension to Wheeler's delayed-choice experiment was realized [10] using the experimental setup shown in fig. 2, which is referred as the delayed-choice quantum eraser experiment (DCQEE), first conceived in 1982 [8] (This paper will refer to [10] as the DCQEE although there have been other papers published that accomplish the essence of a DCQEE experiment [11],[12]). The experiment used four devices D_0, D_1,D_2,D_3 that detected pairs of entangled photons produced at points A or B, where one photon from each pair produced at either A or B ended up in D_0; one photon from the pair created at A ended up at either D_3 or one of the two detectors D_1, D_2, and one photon from the pair created at B was detected at either D_1 or D_2. When one of the entangled photons from A was detected at D_3, the corresponding entangled photon that went to D_0 also was detected WITHOUT interference with any information from B reaching D_0, when the device sampled points along the x-direction, as it would be typical of a double slit experiment. In contrast, when photons were detected at either D_1 or D_2, which detected photons from A or B without knowing if the detection was from one or the other, their corresponding entangled photon at D_0 registered an interference pattern. From a theoretical perspective, three joint probability counts $R_{0,3}$,$R_{0,2}$,$R_{0,1}$ described the results obtained by the experiment [ ]:

$$R_{0,3} \propto \int_0^T \int_0^T dT_0 \, dT_3 \, | \psi (t_0,t_3{}^A)|^2, \qquad (1)$$

$$R_{0,2} \propto \int_0^T \int_0^T dT_0 \, dT_2 \, | \psi (t_0,t_2{}^A)+ \psi (t_0,t_2{}^B)|^2, \qquad (2)$$

and

$$R_{0,1} \propto \int_0^T \int_0^T dT_0 \, dT_1 \, | \psi (t_0,t_1{}^A)+ \psi (t_0,t_1{}^B)|^2 \qquad (3)$$

such that T is the time interval, and the times t_0,t_2,t_3 in the joint wave function were given by $t_i=T_i-L_i/c$ (i=0,1,2,3), where T_i was the detection time for the detectors D_i, and L_i were the optical path lengths from A or B to the detector D_i [ ]. By inspection, it is clear that $R_{0,3}$ did not result in an interference pattern, which was confirmed by

the experiment, given that the integrand corresponds to the probability of joint wave functions for a photon from A only; in contrast, $R_{0,2}$ and $R_{0,1}$ have superposed wave functions in their integrands that originated from both A and B, whose phase differences resulted in wave-like patterns [ ]. Because $L_0 < L_3$, $L_3 < L_1$, $L_3 < L_2$, the measured detection coincidences with D_0, D_1, D_2, D_3 did not correspond to the times t_0, t_1, t_2, t_3 in the theoretical expressions for the joint probability counts $R_{0,3}$, $R_{0,2}$, $R_{0,1}$. Consequently, the joint wave functions that resulted in detection coincidences in all four detectors did not occur simultaneously, but corresponded to different time shifts L_0/c , L_1/c , L_2/c , L_3/c because of the time necessary for photons to arrive to D_0, D_1, D_2, D_3, from A or B, with different optical path lengths. The joint wave functions can be written [ ],

$$\psi(t_i, t_?) \propto \exp[-\Omega_i t_i - \Omega_? t_?] \qquad (4)$$

which does not vanish when $t_i - t_?$ was in the range $0 < t_i - t_? < (L/\mu_i) - (L/\mu_?)$; μ_i and $\mu_?$ were the respective group velocities.
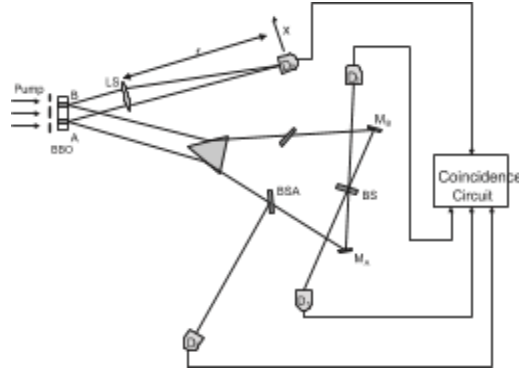

figure 2. Setup for the delayed-choice quantum eraser experiment: detector D_0 sampled points along the x-direction; coincidences with detectors D_1, D_2, D_3 showed that only coincidences with detector D_1, D_2 resulted in an interference-like pattern for different values of x; in contrast, coincidences with D_3 resulted in a gaussian-like distribution along the x-direction; D_0 was measured first because the optical path length from A or B to D_0 was the shortest. (Picture presented in the original paper "A Delayed Choice Quantum Eraser" [9])

Now, the experimental demonstration of Wheeler's delayed-choice experiment with a quantum computer has been recently demonstrated with an IBM quantum computer [14]. fig. 3 shows schematically the circuit that was used to obtain measurements of q[0] when it was in state

$$S1 \propto |0>_0 + e^{i\varphi}|1>_0, \qquad (5)$$

and when the controlled Hadamard gate transformed S1 into the state

$$S2 \propto D(\phi)|0>_0 + F(\phi)|1>_0, \qquad (6)$$

where

$$|D(\phi)|^2 \propto \cos^2(\phi/2) \qquad (7)$$
$$\text{and } |F(\phi)|^2 \propto \sin^2(\phi/2); \qquad (8)$$

thus, S1 provided the "which path information" for either state $|0>_0$ or $|1>_0$, and S1 gave an interference pattern, associated with "wave behavior", such that the state for q[0] was $\psi_0 \propto |0>_0 + e^{i\varphi}|1>_0$ or $\psi_1 \propto |0>_1 - e^{i\varphi}|1>_1$. In this way, the history of q[0], in either state ψ_0 or ψ_1, could be $\psi_0 \propto |0>_0$ or $\psi_1 \propto |0>_1$ when q[0] was operated by the Hadamard gate and U1(ϕ) only; however, when the additional control hadamard gate was applied, the state of q[0] became either $\psi_0 \propto |0>_0 + e^{i\varphi}|1>_0$ or $\psi_1 \propto |0>_1 - e^{i\varphi}|1>_1$. Now, in the same paper, a further development to Wheeler's thought experiment was presented, which is shown fig. 4 [15]; like the

previous example, states S1 and S2 were created as well, but the outcomes were rotated by a U3 gate AFTER the state S1 or S2 were formed, resulting in an entanglement

$$| E >= \sum_{i,j,k}^{0,1} C_{q[0], q[1], q[2]} \cdot |i>_{q[0]} \otimes |j>_{q[1]} \otimes |k>_{q[2]} \tag{9}$$

where $\cdot$ and $\otimes$ are the number product and the tensor product respectively; i,j,k, in the summation, could take the value 0 or 1, and $C_{q[0], q[1], q[2]}$ was a number that depended on the settings for U1(ϕ) on q[0] and the settings for U3(θ, ϕ, λ) on q[2]; thus, measurements on q[0] and q[2] were "space-like" separated and did not have to happen at the same time, which was an extension of wheeler's delayed-choice thought experiment.
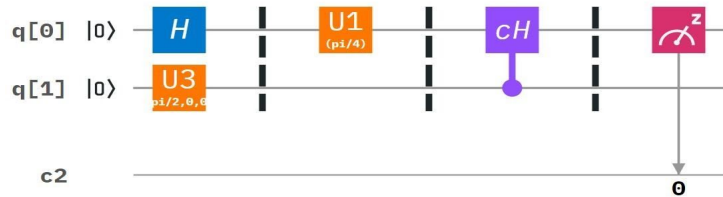

figure 3. Computerized version of Wheeler's Delayed-choice quantum thought experiment. (Picture from "Demonstration of quantum delayed-choice experiment on a quantum computer" [13])
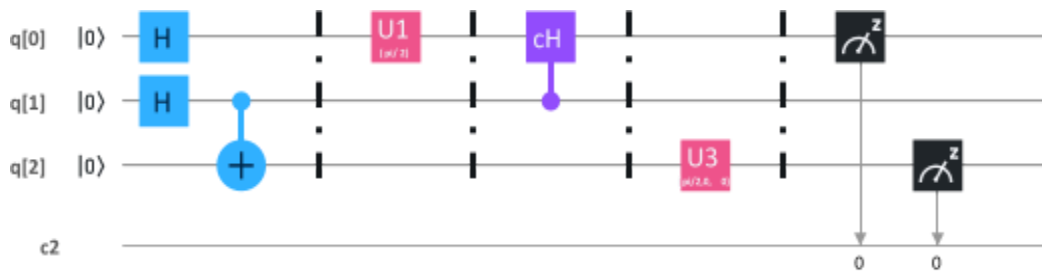

figure 4. Computerized version of an entanglement-assisted quantum delayed-choice experiment. (Picture also from "Demonstration of quantum delayed-choice experiment on a quantum computer" [13])

Extending the previous work, we present a DCQEE, shown on fig 6-7, on an IBM quantum computer, where the state of q[0] led to an interference pattern only in relation to some remote qubits but not in relation to others, and measurements of q[0] took place BEFORE the other qubits, allowing to interpret the remote post-measurements as "erasing" the previous history of q[0]. In the DCQEE, the detectors for the "which path" information (D_0, D_1, D_2) and the detectors that gave an interference pattern (D_0,D_3) shared one detector (D_0) that was closer to the source than the other other detectors, allowing it to make detections BEFORE detectors D_0, D_1, D_2, which were implied by the optical path lengths traveled. Similarly, given that the IBM quantum computer used for the present experiment was capable of making measurements in an orderly way at the end of each run of an experiment, where measurements on q[0] were done first, as shown in the experimental set up in fig 6-7, as well as in the corresponding transpiled circuit in fig 9-10, a quantum computer version of the DCQEE was possible: the measuring device on q[0], with its output on qubit c[0], was homologous to D_0; the measuring device on q[4] (with

or without q[3]), whose output ended on c[4] (with or without c[3]) occurred AFTER c[0] was recorded, and was homologous to either detector D_1 or D_2 in DCQEE; the output on c[1], from the measuring device on q[1], detected the "which path" information, and was homologous to the detector D_3. It is important to note that measurements on each of the qubits alone could NOT have detected any phase value changes set in any of the U1 gates in the circuit. All relevant qubits had to be measured to make a detection of an interference pattern i.e. at least, q[0] had to be measured with q[4] in order to detect an interference pattern by multiple measurements with different phase values (fig. 6). In this way, the interference pattern that was obtained with the phase values set manually in all U1 gates was the result of joint measurements with the other qubits in an entanglement of the form

$$|G> = \sum_{i,j,k,l,m}^{0,1} C_{i,j,k,l,m} \cdot |i>_{q[0]} \otimes |j>_{q[1]} \otimes |k>_{q[2]} \otimes |l>_{q[3]} \otimes |m>_{q[4]} \qquad (10)$$

where i,j,k,l,m could take the values 0 or 1 in the summation, and $C_{i,j,k,l,m}$ depended on the value set on all the U1 gates on q[0] and q[3] (but only the U1 gate at q[3] led to an interference-like pattern). Note that $|G>$ could be written in multiple ways by associating the five complex coefficients that belong to the set $K = \{ \xi^{(n)}_{i,j,k,l,m} / n=0,1,2,3,4 \wedge C_{i,j,k,l,m} = \xi^{(0)}_{i,j,k,l,m} \cdot \xi^{(1)}_{i,j,k,l,m} \cdot \xi^{(2)}_{i,j,k,l,m} \cdot \xi^{(3)}_{i,j,k,l,m} \cdot \xi^{(4)}_{i,j,k,l,m} \}$ with their respective state-factors in the entanglement i.e.

$$|G> = \sum_{i,j,k,l,m}^{0,1} (\xi^{(0)}_{i,j,k,l,m} \cdot |i>_{q[0]}) \otimes (\xi^{(1)}_{i,j,k,l,m} \cdot |j>_{q[1]}) \otimes (\xi^{(2)}_{i,j,k,l,m} \cdot |k>_{q[2]})$$
$$\otimes (\xi^{(3)}_{i,j,k,l,m} \cdot |l>_{q[3]}) \otimes (\xi^{(4)}_{i,j,k,l,m} \cdot |m>_{q[4]}). \qquad (11)$$

Consequently, the expression $<G|\odot|G>$, where $\odot$ is the dot product, can be written,

$$<G|\odot|G> = \sum_{i,j,k,l,m}^{0,1} \sum_{i,j,k,l,m}^{0,1} <i'|_{q[0]} \, \xi^{(0)*}_{i,j,k,l,m'} \odot \xi^{(0)}_{i,j,k,l,m} |i>_{q[0]} \cdot$$
$$<j'|_{q[1]} \, \xi^{(1)*}_{i,j,k,l,m'} \odot \xi^{(1)}_{i,j,k,l,m} |j>_{q[1]} \cdot$$
$$<k'|_{q[2]} \, \xi^{(2)*}_{i,j,k,l,m'} \odot \xi^{(2)}_{i,j,k,l,m} |k>_{q[2]} \cdot$$
$$<l'|_{q[3]} \, \xi^{(3)*}_{i,j,k,l,m'} \odot \xi^{(3)}_{i,j,k,l,m} |l>_{q[3]} \cdot$$
$$<m'|_{q[4]} \, \xi^{(4)*}_{i,j,k,l,m'} \odot \xi^{(4)}_{i,j,k,l,m} |m>_{q[4]}, \qquad (12)$$

$$\text{where } {}_{q[n]}<\alpha'|\odot|\alpha>_{q[n]} = \delta_{\alpha',\alpha} \text{ for } \alpha' \text{ and } \alpha = \{0,1\};$$

in this way, the probabilities for each term in the dot product $<G|\odot|G>$ is given by $\xi^{(n)*}_{i,j,k,l,m} \cdot \xi^{(n)}_{i,j,k,l,m}$, where each probability can be interpreted to be the result of individual qubits in superpositions $\xi^{(n)}_{i,j,k,l,m}|\alpha>_{q[n]} = A^{(n)}(\phi_1^{(n)})|\alpha>_{q[n]} + B^{(n)}(\phi_2^{(n)})|\alpha>_{q[n]}$, but the phase differences, $\Delta\phi^{(n)} = \phi_2^{(n)} - \phi_1^{(n)}$, were not necessarily the result of operations performed on q[n], which, nevertheless, manifested on q[n] because of the entanglement with the other qubits where such operations could affect the state of those other qubits directly; for the present experiment, the phase value $\phi^{q[3]}$ in the controlled $U1^{q[3]}$ gate, on q[3], necessarily produced an interference-like pattern for some $\xi^{(n)}_{i,j,k,l,m}$ contrasting the effect that the phase value in the controlled $U1^{q[0]}$ gate on q[0] had on any $\xi^{(n)}_{i,j,k,l,m}$, which by itself could not have created an interference pattern i.e. $\exists \, \xi^{(n)}_{i,j,k,l,m}$ such that $|\xi^{(n)}_{i,j,k,l,m}[U1^{q[3]}(\phi^{q[3]})]|^2 \propto \cos^2(\phi^{q[3]}/2)$ or $\propto \sin^2(\phi^{q[3]}/2)$. The interpretation in this paper is that $C_{i,j,k,l,m} = \xi^{(0)}_{i,j,k,l,m}$, which entails that $\xi^{(1)}_{i,j,k,l,m} = \xi^{(2)}_{i,j,k,l,m} = \xi^{(3)}_{i,j,k,l,m} = \xi^{(4)}_{i,j,k,l,m} = 1$; therefore, in this interpretation, q[0] was the only qubit that was in a superposition state that resulted in the interference-like pattern when it was entangled with the other qubits in such a way that $|C_{i,j,k,l,m}|^2$ was dependent on $\Delta\phi$ in $|G>$. from an empirical perspective, only when multiple joint measurements on q[0] with q[4] were included, an interference-like pattern was detectable by changing the value of $\phi^{q[3]}$, allowing to attribute the interference pattern to the measuring device on q[0] and treating the other as a detecting device; nevertheless, q[0]'s measuring device could have been treated as the detector as well. Also, in the DCQEE, is possible to interpret the interference-like pattern observed

when joint detections occurred in D_0 together with D_1 or D_2 as the result of phase differences in any of the detectors (where the difference is a function of sampling points on the x direction with D_0) by writing the superposition of two joint wave functions as the product of individual wave functions and associating the coefficient with one of the state-factors:

$$\psi(t_0,t_1{}^A)+\psi(t_0,t_1{}^B) \propto C_{D_0,D_1}\cdot\exp[-\Omega_0 t_0]\cdot\exp[-\Omega_1 t_1]$$

$$= \xi^{(0)}{}_{D_0,D_1}\cdot\exp[-\Omega_0 t_0]\cdot \xi^{(1)}{}_{D_0,D_1}\cdot\exp[-\Omega_1 t_1] \tag{13}$$

and

$$\psi(t_0,t_2{}^A)+\psi(t_0,t_2{}^B) \propto C_{D_0,D_2}\cdot\exp[-\Omega_0 t_0]\cdot\exp[-\Omega_2 t_2]$$

$$= \xi^{(0)}{}_{D_0,D_2}\cdot\exp[-\Omega_0 t_0]\cdot \xi^{(1)}{}_{D_0,D_1}\cdot\exp[-\Omega_2 t_2]\,, \tag{14}$$

where $C_{D_0,D_2} = \xi^{(0)}{}_{D_0,D_2}\cdot \xi^{(2)}{}_{D_0,D_2}$ and $C_{D_0,D_1} = \xi^{(0)}{}_{D_0,D_1}\cdot \xi^{(2)}{}_{D_0,D_1}$; by setting $C_{D_0,D_2} = \xi^{(2)}{}_{D_0,D_2}$ or $C_{D_0,D_1} = \xi^{(1)}{}_{D_0,D_1}$, the phase differences creating the interference pattern can be interpreted to happen at detectors D_1 or D_2 rather than D_0 (as is not usually conceived in double slit experiments) but such a phase difference is a function of the x-position of D_0 i.e $|\xi^{(2)}{}_{D_0,D_2}[\Delta\phi^{(2)}(x)]|^2$ or $|\xi^{(1)}{}_{D_0,D_1}[\Delta\phi^{(1)}(x)]|^2$.

To produce an interference pattern, in this computerized version of the DCQEE, and contrast it with a non-interference pattern, using q[0] as the target qubit with other qubits that served as detectors, multiple measurements on q[1], q[2], q[3], and q[4], while being entangled with q[0] in state

$$|E1> \propto |0>_0|1>_1|0>_2|0>_3|0>_4 + e^{i\varphi}|1>_0|0>_1|0>_2|0>_3|0>_4 \tag{15}$$

or

$$|E2> \propto d(\phi)|0>_0|0>_1|1>_2|+>_3|1>_4 +$$
$$f(\phi)|1>_0|0>_1|1>_2|->_3|1>_4 +$$
$$g(\phi)|0>_0|0>_1|1>_2|->_3|0>_4 +$$
$$h(\phi)|1>_0|0>_1|1>_2|+>_3|0>_4 \tag{16}$$

were done. Starting at the top fig. 6, multiple measurements on q[1], while being entangled with q[0] in $|E1>$, served to obtain a non-interference pattern (constant probability as the phase value $\phi^{q[0]}$ was changed in the $U1^{q[0]}$ gate) AFTER the state of q[0] was formed that could be attributed to q[0] for every result obtained at q[1] as either "1" ($|1>_1$) when q[0] was in state $|0>_0$, or "0" ($|0>_1$) when q[0] was in state $|1>_0$. Measurements on q[0] were done first in any joint measurement with the other qubit. The interference pattern happened when the second state $|E2>$ was activated (when q[2] was in state $|1>_2$), where the outcome of the quantum gates on q[0], was also necessary BEFORE being entangled with other qubits; however, $|E2>$ resulted in an interference-like pattern when multiple measurements on q[0] were performed together with other relevant qubits, much like, in the DCQEE, multiple joint measurements on D_0 with D_1,D_2 were performed and resulted in an interference-like pattern as D_0 sampled points along the x direction. In this way, multiple measurements produced an interference pattern only as a result of the entanglement $|E2>$ that allowed to interpret the measurements on q[0] as an interference pattern (a superposition of two equal states with a phase difference) happening on the measuring device on q[0], that did not exist BEFORE the sequence of measurements were performed with the remote qubit q[4] (with or without q[3]) i.e. $d(\phi)$, $f(\phi)$, $g(\phi)$, $h(\phi)$ are complex numbers that could be associated with any of the state-factors in each of the terms of $|E2>$; only a series of measurements on q[0] and q[4] (and q[2] which signaled when $|E2>$ was "activated") were sufficient to determine an interference like probability (measurements

on q[3] complemented the measurements on q[0] and q[4], but did not change the probability as a function of the phase value ϕ set in any U1 gate, which can be seen by comparing the results from fig. 13(A)-(B) with 14(A)). It is important to mention that q[2] merely activated either |E1> and |E2>, simulating a one quantum system that allowed q[0] to behave as a "particle" in states $\{(1/\sqrt{2})|0>_0$, $(1/\sqrt{2})e^{i\varphi}|1>_0\}$, or as "waves" $\{A_0(\phi)|0>_0+B_0(\phi)|0>_0,\ C_0(\phi)|1>+D_0(\phi)|0>_0\}$; on the other hand, any of the qubits involved in the entanglement |E2> could have been interpreted as "waves" in the same way, by associating the coefficient of each computational basis element with a factor in the tensor product, but only the measurements on q[0] resulted in two possible outcomes, either $|0>_0$ or $|1>_0$, in both entanglements |E1> and |E2>, by multiple measurements; moreover, q[0] was measured before the other qubits when joint measurements were performed (any qubit had to be measured first). Now, to quantify the variability of the multiple measurements, the formula

$$\text{Variability=(maximum probability - minimum probability) / Average probability} \qquad (17)$$

was used; calculations with multiple measurements of q[0], with q[1], when |E1> was activated (q[2] was in state $|0>_0$), showed a variability of less than 1. In contrast, when multiple measurements on both q[0] and q[4] (with or without q[3]) were done, while |E2> was activated (q[2] was in state $|1>_1$), the variability of the multiple measurements was greater than 1; moreover, the shape of the data, as a function of the phase value $\phi^{q[3]}$, resembled consistently the shape of $\propto \cos^2(\phi^{q[3]}/2)$ or $\propto \sin^2(\phi^{q[3]}/2)$ (blue pattern in fig. 12(A)-(D)) as expected by theory, contrasting the fluctuating pattern obtained when when q[0] and q[1] were measured in entanglement |E1> (orange pattern in fig. 12(A)-(D)).

METHOD

Using an IBM quantum computer (VIGO) a general entanglement G was created using 5-qubits as shown on fig. 6-8:

$$|G> = (1/\sqrt{2})\, Z_1\, (|0>_0|1>_1|0>_2|0>_3|0>_4 + e^{i\varphi}|1>_0|0>_1|0>_2|0>_3|0>_4)+$$

$$(1/\sqrt{2})\, Z_2\, [(1+e^{i\phi})|0>_0|0>_1|1>_2|0>_3|1>_4 + (1-e^{i\phi})(e^{i\phi})|1>_0|0>_1|1>_2|0>_3|1>_4 +$$

$$(1+e^{i\phi})|0>_0|0>_1|1>_2|1>_3|1>_4 - (1-e^{i\phi})(e^{i\phi})|1>_0|0>_1|1>_2|1>_3|1>_4 +$$

$$(1-e^{i\phi})|0>_0|0>_1|1>_2|0>_3|0>_4 + (1+e^{i\phi})(e^{i\phi})|1>_0|0>_1|1>_2|0>_3|0>_4 +$$

$$-(1-e^{i\phi})|0>_0|0>_1|1>_2|1>_3|0>_4 + (1+e^{i\phi})(e^{i\phi})|1>_0|0>_1|1>_2|1>_3|0>_4]. \qquad (18)$$

The subscripts in the expression corresponded to the qubits q[0],q[1],q[2],q[3],q[4], and all states in the entanglement G were in the z-basis, and the tensor product symbol has been dropped but it is implied to be the product among the state-factors. (Notice that only one phase value ϕ was used in the expression; the reason is that all U1 gates were set to the same value ϕ in all the experiments performed.) A simpler way to write |G> is to write it in terms of two entanglements:

$$|E1>=(1/\sqrt{2})\, Z_1\, (|0>_0|1>_1|0>_2|0>_3|0>_4 + e^{i\phi}|1>_0|0>_1|0>_2|0>_3|0>_4) \qquad (19)$$

$$|\, E2>=(1/\sqrt{2})\, Z_2\, [(1+e^{i\phi})|0>_0|0>_1|1>_2|0>_3|1>_4 + (1-e^{i\phi})(e^{i\phi})|1>_0|0>_1|1>_2|0>_3|1>_4 +$$

$$(1+e^{i\phi})|0>_0|0>_1|1>_2|1>_3|1>_4 - (1-e^{i\phi})(e^{i\phi})|1>_0|0>_1|1>_2|1>_3|1>_4 +$$

$$(1-e^{i\phi})|0>_0|0>_1|1>_2|0>_3|0>_4 + (1+e^{i\phi})(e^{i\phi})|1>_0|0>_1|1>_2|0>_3|0>_4 +$$

$$-(1-e^{i\phi})|0\rangle_0|0\rangle_1|1\rangle_2|1\rangle_3|0\rangle_4+(1+e^{i\phi})(e^{i\phi})|1\rangle_0|0\rangle_1|1\rangle_2|1\rangle_3|0\rangle_4]. \qquad (20)$$

In this way, one may easily notice that the outcome of the measurements on q[2] determined the way q[0] was entangled. Notice that when states $\{..|1\rangle_1|0\rangle_2..., ...|0\rangle_1|0\rangle_2...\}$ were measured, the corresponding outcomes measured on q[0] were $\{|0\rangle_0...., |1\rangle_0.....\}$ with equal and uniform probability regardless of the phase value; consequently, multiple measurements (1000 shots) of q[0] and q[1] were done to quantify the variability of elements of the computational basis that contain the string $\{..|1\rangle_1|0\rangle_2..., ...|0\rangle_1|0\rangle_2...\}$ by placing measuring devices on q[0] and q[1] (and q[2]) . Also, it may be easily noticed that |G> implied eight superposition states, four for $|0\rangle_0$ and four for $|1\rangle_0$, when the computational basis elements contain the strings,

$$\{...|0\rangle_2|0\rangle_3|1\rangle_4 , ...|0\rangle_2|1\rangle_3|1\rangle_4 , ...|0\rangle_2|0\rangle_3|0\rangle_4 , ...|0\rangle_2|1\rangle_3|0\rangle_4\}. \qquad (21)$$

Because the phase differences ϕ implied a probability as a function of the phase value for all eight superpositions, the program was run by setting phase values manually in all the corresponding gates (U1 gates on q[0] and q[3]), in the range (0,2*pi), in increments of 0.5pi/4. Notice that in the experimental set up (fig 6-8), the state $(1/\sqrt{2})(|0\rangle_0 +e^{i\phi} |1\rangle_0$ was necessary to form |E1> because a CNOT gate was needed to connect the state of q[0] to the outcome of the state on q[4]; also, |E1> required a second CNOT gate to connect the operations on q[3] on q[4] once the outcome of the state $(1/\sqrt{2})(|0\rangle_0 +e^{i\phi}|1\rangle_0$ had controlled over q[4]; in this way, operations on q[0] were not sufficient to produce an interference pattern, but the state of q[0] that resulted from the operations on q[0] was necessary to obtain an interference pattern after forming entanglement |E2>.

As seen on the top left of the circuit diagrams in fig 5-8, a controlled Hadamard and U1(ϕ) gate originated the entanglement $|E1>=(|0\rangle_0|1\rangle_1...+e^{i\phi}|1\rangle_0|0\rangle_1...)$ whenever q[2] was in state $|0\rangle_2$; when both gates were activated, q[0], initially in state $|0\rangle_0$, transformed into the state $Sq[0]\propto|0\rangle_0+e^{i\phi}|1\rangle_0$. Notice that the probability of obtaining either $|0\rangle_0$ or $|1\rangle_0$ was ½ regardless of the value of the phase value ϕ due to the orthogonality of the states; thus, the phase difference in the states $\{|0\rangle_0 ,|1\rangle_0\}$ did not cause an interference pattern when multiple measurements on q[0] were done. To quantify the variability in the measurements, the formula VARIABILITY=(Max Prob.-Min Prob.)/Average prob. was used to quantify the probability as a function of the phase value ϕ when q[0] was measured by itself, expecting VARIABILITY <<1 for the probability of any of the two terms in |E1> for different values of ϕ. Now, multiple measurements (1000 shots) of both q[0] and q[1], when |E1> occurred, gave similar results because the probability of obtaining either $|0\rangle_0|1\rangle_1$ or $|1\rangle_0|0\rangle$ was also ½.

Also, on the top of the circuit, the second controlled Hadamard gate and the controlled U1(ϕ) gate resulted in a state $Sq[0]\propto(|0\rangle_0+e^{i\phi}|1\rangle_0)$ when $|0\rangle_2$ occurred, which was necessary to create the entanglement |E2>. First, q[3] was prepared exactly like q[0], which set it in state $Sq[3]\propto(|0\rangle_3+e^{i\phi}|1\rangle_3)$; then, a controlled Hadamard gate on q[3] created the two states

$$W^{(+)}{}_3 \propto |0\rangle_3+e^{i\phi}|0\rangle_3 \qquad (22)$$

$$\text{and } W^{(-)}{}_3 \propto |1\rangle_3-e^{i\phi}|1\rangle_3. \qquad (23)$$

In this way, before |E2> was formed, the CNOT gate from q[3] into q[4,] and the CNOT gate from q[0] into q[4], allowed to compare the outcomes of states Sq[0] with $W^{(+)}{}_3$ and $W^{(-)}{}_3$. Consequently, q[4] gave "0" when the states from both q[0] and q[3] were the same, and "1" when they were different i.e. q[4] detected

$$d(\phi)|0\rangle_0...|0\rangle_3..+f(\phi)|1\rangle_0...|1\rangle_3.. \qquad (24)$$

when q[4] was in state $|0\rangle_4$, or

$$g(\phi)|0\rangle_0...|1\rangle_3..+h(\phi)|1\rangle_0...|0\rangle_3.. \qquad (25)$$

when q[4] was in state $|1\rangle_4$. One can easily verify that the values of d(ϕ), f(ϕ), g(ϕ), h(ϕ), are given by

$$\{(1+e^{i\phi}), (1-e^{i\phi})(e^{i\phi}), (1-e^{i\phi}), (1+e^{i\phi})(e^{i\phi})\} \qquad (26)$$

respectively, whose absolute squares (complex number times their conjugate) are proportional to

$$\{ \propto \cos^2(\phi/2), \propto \sin^2(\phi/2), \propto \sin^2(\phi/2), \propto \cos^2(\phi/2)\} \qquad (27)$$

respectively. Then, on the bottom right of fig. 5-8, there is a second controlled Hadamard gate on q[3] that transforms $|0>_3$ into $|+>_3$ and $|1>_3$ into $|->_3$, where $|+>_3=(1/\sqrt{2})(|0>_3+|1>_3)$ and $|->_3=(1/\sqrt{2})(|0>_3-|1>_3)$; doing so finally leaves q[0],q[3],q[4] in state

$$|E2> = d(\phi)|0>_0...|+>_3|1>_4+f(\phi)|1>_0...|->_3|1>_4+$$

$$g(\phi)|0>_0...|->_3|0>_4+h(\phi)|1>_0...|+>_3|0>_4. \qquad (28)$$
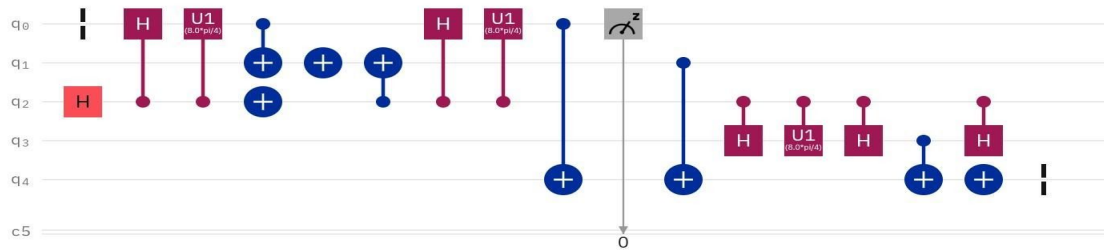
figure 5. Experimental setup for a computerized version of the DCQEE with only measurements on q[0]; the phase value in all U1 gates was varied; the same phase value was set in all U1 gates for each run of the experiment. All measurements were delivered on qubit c[0]
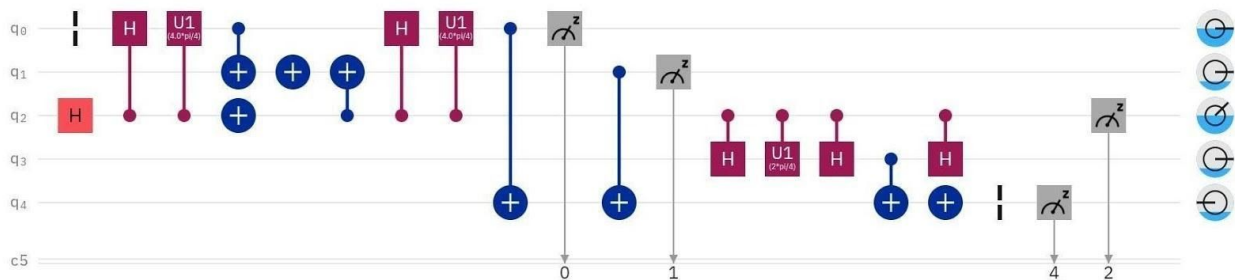

figure 6. Experimental setup for a computerized version of the DCQEE with measuring devices on q[0], q[1], q[2], and q[4]; the phase value in all U1 gates was varied; the same phase value was set in all U1 gates for each run of the experiment. All measurements were delivered on qubits c[0], c[1], c[2], c[4] respectively.

Now, for simplicity, only multiple measurements on q[0] were done first. Then, multiple measurements with q[0] and q[4] were done without q[3]; from the expression for |E1> follows that when measurement in the computational basis elements included the strings

$$\{|0>_0....|1>_4, |1>_0....|1>_4, |0>_0....|0>_4, |1>_0...|0>_4\} \qquad (29),$$

the corresponding coefficients were

$$\{d(\phi), f(\phi), g(\phi), h(\phi)\} \qquad (30)$$

respectively. Given the probabilities for each string was given by

$$|d(\phi)|^2 \propto \cos^2(\phi/2),$$

$$|f(\phi)|^2 \propto \sin^2(\phi/2),$$

$$|g(\phi)|^2 \propto \sin^2(\phi/2),$$

$$\text{and } |h(\phi)|^2 \propto \cos^2(\phi/2), \qquad (31)$$

but measurements on q[0] and q[1] were not functions of the phase value ϕ, multiple measurements with q[0], q[1], q[2], q[4], while changing the phase value ϕ, allowed to obtain the probability for the set of basis elements (29) as a function of ϕ and compare the probability function with the outcomes of q[0] and q[1] in state |E1>, where the possible outcomes were

$$\{|0>_0|1>_1|0>_2 ..., |1>_0|0>_1|0>_2 ...\}, \qquad (33)$$

which were expected to be constant in regards to changes in phase values ϕ done manually in all the U1 gates. The outcomes from q[2] allowed to distinguish in the computational basis when the set $\{|0>_0|1>_1|0>_2....,|1>_0|0>_1|0>_2....\}$ was obtained (E1 activated) or when the set $\{|0>_0...|0>_2...|1>_4, |1>_0...|0>_2...|1>_4, |0>_0...|0>_2...|0>_4, |1>_0...|0>_2...|0>_4\}$ was obtained (E2 activated). The variability of the probability obtained when both sets were detected, as well as their graphs as function of the phase value, were contrasted to distinguish their features, and be able to validate that both entanglements |E1>and |E2> remained coherent and measurements were consistent with calculations.
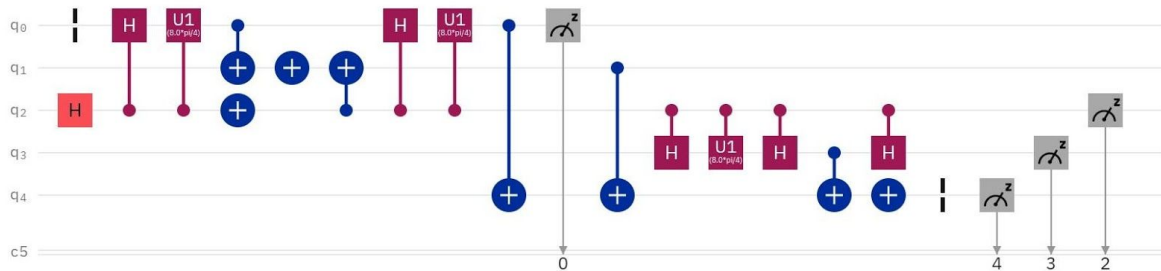

figure 7. Experimental setup for a computerized version of the DCQEE with measuring devices on q[0], q[2], q[3], and q[4]; the phase value in all U1 gates was varied; the same phase value was set in all U1 gates for each run of the experiment. All measurements were delivered on qubits c[0], c[2], c[3], and c[4] respectively.

Now, when q[3] was measured in the z-basis, together with q[0] and q[4], eight possible interference patterns were obtained as a result of multiple measurements (1000 shots). This can be easily discerned by taking the

entanglement $|E2\rangle = d(\varphi)|0\rangle_0\,|0\rangle_1\,|1\rangle_2|+\rangle_3|1\rangle_4 + f(\varphi)\,|1\rangle_0\,|0\rangle_1\,|1\rangle_2\,|-\rangle_3|1\rangle_4 + g(\varphi)|0\rangle_0\,|0\rangle_1\,|1\rangle_2\,|-\rangle_3\,|0\rangle_4$ $+h(\varphi)|1\rangle_0\,|0\rangle_1\,|1\rangle_2|+\rangle_3|0\rangle_4$, and writing it all in the z-basis, which gives

$$|E2\rangle \propto d(\phi)|0\rangle_0..(|0\rangle_3+|1\rangle_3)|1\rangle_4 +$$

$$f(\phi)|1\rangle_0...(|0\rangle_3-|1\rangle_3)|1\rangle_4 +$$

$$g(\phi)|0\rangle_0...(|0\rangle_3-|1\rangle_3)|0\rangle_4 +$$

$$h(\phi)|1\rangle_0...(|0\rangle_3+|-\rangle_3)|0\rangle_4 . \qquad (34)$$

By multiplying and rearranging terms, $|E2\rangle$ becomes

$$\propto (1+e^{i\phi})|0\rangle_0|0\rangle_1|1\rangle_2|0\rangle_3|1\rangle_4+(1-e^{i\phi})(e^{i\phi})|1\rangle_0|0\rangle_1|1\rangle_2|0\rangle_3|1\rangle_4 +$$

$$(1+e^{i\phi})|0\rangle_0|0\rangle_1|1\rangle_2|1\rangle_3|1\rangle_4-(1-e^{i\phi})(e^{i\phi})|1\rangle_0|0\rangle_1|1\rangle_2|1\rangle_3|1\rangle_4 +$$

$$(1-e^{i\phi})|0\rangle_0|0\rangle_1|1\rangle_2|0\rangle_3|0\rangle_4+(1+e^{i\phi})(e^{i\phi})|1\rangle_0|0\rangle_1|1\rangle_2|0\rangle_3|0\rangle_4 +$$

$$-(1-e^{i\phi})|0\rangle_0|0\rangle_1|1\rangle_2|1\rangle_3|0\rangle_4+(1+e^{i\phi})(e^{i\phi})|1\rangle_0|0\rangle_1|1\rangle_2|1\rangle_3|0\rangle_4$$

From this expression follows that when the strings in the computational basis contained $\{...|0\rangle_3|1\rangle_4|0\rangle_0$, $...|1\rangle_3|1\rangle_4|0\rangle_0$, $...|0\rangle_3|0\rangle_4|0\rangle_0$, $...|1\rangle_3|0\rangle_4|0\rangle_0$, $...|0\rangle_3|1\rangle_4|1\rangle_0$, $...|1\rangle_3|1\rangle_4|1\rangle_0$, $...|0\rangle_3|0\rangle_4|1\rangle_0$, $...|1\rangle_3|0\rangle_4|1\rangle_0,\}$, one of the eight complex coefficients was associated with q[0], making the probability for each of the eight possibilities equal to the absolute square of its corresponding coefficient; 1000 shots per run of each experiment, for each phase value φ, in steps of $0.5\pi/4$, in the range $(0, 2\pi)$, were done by measuring q[0], q[2], q[3], q[4], where q[2] only served to detect "1" in the computational basis to indicate that entanglement E2 was activated. A plot of the probability for each outcome as a function of the phase value was created to identify characteristic features of each absolute square of the eight complex coefficients.
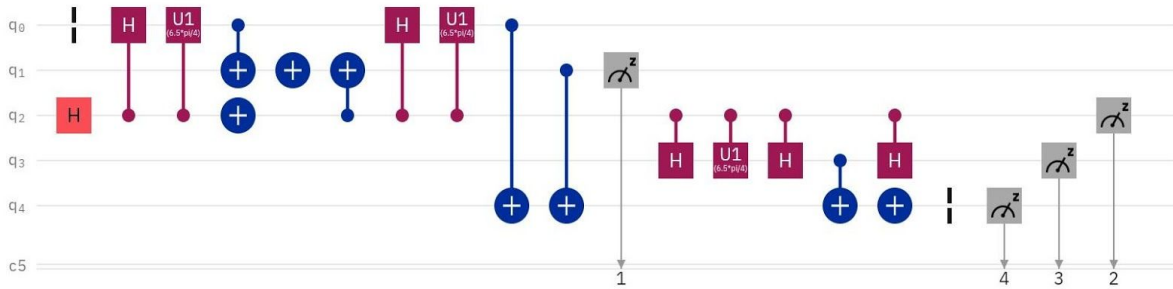

figure 8. Experimental setup for a computerized version of the DCQEE with measuring devices on q[1], q[2], q[3], and q[4]; the phase value in all U1 gates was varied; the same phase value was set in all U1 gates for each run of the experiment. All measurements were delivered on qubits c[1], c[2], c[3], and c[4] respectively.

To contrast the previous results, only the states of q[3] and q[4] were measured in the z-basis to show that the phase φ did not manifest (probability NOT a function of ϕ) when multiple measurements of those qubits were done without the measurements of the state of q[0]. Notice that by detecting only any of the strings $\{....|0\rangle_3|1\rangle_4$, $....|1\rangle_3|1\rangle_4$, $...|0\rangle_3|0\rangle_4$, $...|1\rangle_3|0\rangle_4\}$ in the computational basis , using the circuit shown in fig. 8, (without the any specific quantum information from q [0]), four possible states can be interpreted for q[0]:

$$\{(1+e^{i\phi})|0\rangle_0+(1-e^{i\phi})(e^{i\phi})|1\rangle_0,$$

$$(1+e^{i\phi})|0>_0-(1-e^{i\phi})(e^{i\phi})|1>_0,$$

$$(1-e^{i\phi})|0>_0+(1+e^{i\phi})(e^{i\phi})|1>_0,$$

$$-(1-e^{i\phi})|0>_0+(1+e^{i\phi})(e^{i\phi})|1>_0\};\qquad\qquad (35)$$

by the orthogonality of the states $|0>_0$, $|1>_0$, and the fact the absolute square of their coefficients is either $\cos^2(\phi/2)$ or $\sin^2(\phi/2)$, where each pair of terms in the four expressions have one of both, and together with the relation $\cos^2(\phi/2)+\sin^2(\phi/2)=1$, one may deduce that the probability of obtaining ….$|0>_3|1>_4$, …$|1>_3|1>_4$,…$|0>_3|0>_4$, or ….$|1>_3|0>_4$ in the computational basis for the setup in fig. 8 was independent of the phase value ϕ i.e. the theoretical value of the variability for the probability to obtain ….$|0>_3|1>_4$, ….$|1>_3|1>_4$, …$|0>_3|0>_4$, or …$|1>_3|0>$ by changing ϕ, was 0, because their probabilities remained constant when $|E2>$ happened:

$$|\propto (1+e^{i\phi})|0>_0|0>_1|1>_2|0>_3|1>_4+(1-e^{i\phi})(e^{i\phi})|1>_0|0>_1|1>_2|0>_3|1>_4|^2 =$$

$$|\propto (1+e^{i\phi})|0>_0|0>_1|1>_2|1>_3|1>_4-(1-e^{i\phi})(e^{i\phi})|1>_0|0>_1|1>_2|1>_3|1>_4|^2 =$$

$$|\propto (1-e^{i\phi})|0>_0|0>_1|1>_2|0>_3|0>_4+(1+e^{i\phi})(e^{i\phi})|1>_0|0>_1|1>_2|0>_3|0>_4|^2 =$$

$$| \propto -(1-e^{i\phi})|0>_0|0>_1|1>_2|1>_3|0>_4+(1+e^{i\phi})(e^{i\phi})|1>_0|0>_1|1>_2|1>_3|0>_4 |^2=$$

$$\text{constant (i.e. independent of } \phi),$$

$$(36)$$

which indicated that the phase value did not have an effect in the probability outcome when measuring devices were set on q[3] and q[4] only i.e. measuring only q[3] and q[4] did not allow to know whether q[0] was |0> or |1> which implies that the probability of any state that contained a specific string from q[3] and q[4] had to be superposed before finding the absolute square [4]; furthermore, it is possible to generalize, from the previous statement, that by having a measuring device only on q[3], no interference pattern could have been detected; the same can be stated about measurements on q[4] alone. Paradoxically, when measuring devices were set on q[0] together with q[3] and q[4], an interference pattern was detected. In fact measuring devices on q[0] and q[4] were sufficient to obtain a probability as a function of the phase ϕ, whereas measuring only q[3] and q[4] were not; this can also be easily implied from the fact that,

$$|(1+e^{i\phi})|0>_0|0>_1|1>_2|0>_3|1>_4|^2=|(1+e^{i\phi})|0>_0|0>_1|1>_2|1>_3|1>_4|^2$$

$$|(1-e^{i\phi})(e^{i\phi})|1>_0|0>_1|1>_2|0>_3|1>_4|^2 = |-(1-e^{i\phi})(e^{i\phi})|1>_0|0>_1|1>_2|1>_3|1>_4|^2$$

$$|(1-e^{i\phi})|0>_0|0>_1|1>_2|0>_3|0>_4|^2 = |-(1-e^{i\phi})|0>_0|0>_1|1>_2|1>_3|0>_4|^2$$

$$|(1+e^{i\phi})(e^{i\phi})|1>_0|0>_1|1>_2|0>_3|0>_4|^2= |(1+e^{i\phi})(e^{i\phi})|1>_0|0>_1|1>_2|1>_3|0>_4|^2,\qquad (37)$$

which shows that the state of q[3] does not have an effect on the probability for the computational basis elements when $|E2>$ was activated. In this way, 1000 shots of the circuit were done by measuring only q[3],q[4] (with q[2], which serve identify when E2 was activated), while manually changing the phase value ϕ of the U1 gate, every 1000 shots (after each run of the program); the multiple measurements determined the probability for each phase value and were plotted; variability was calculated.
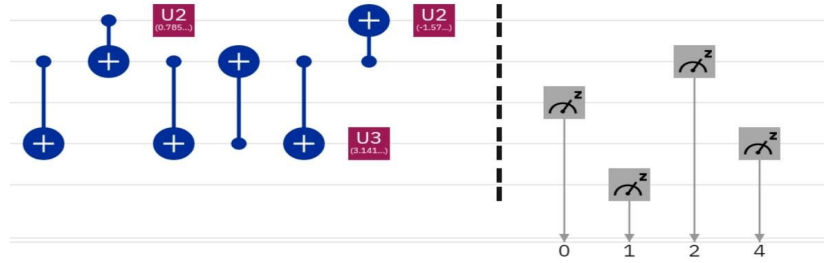
figure 9. Portion of the transpiled circuit corresponding to figure 6. (diagram continues to the left). Measurements were done at the end of each run of the experiment, but measurements on q[0] were done first (followed by q[1], q[2], q[4]); however, the exact time for the measurements was not determined.
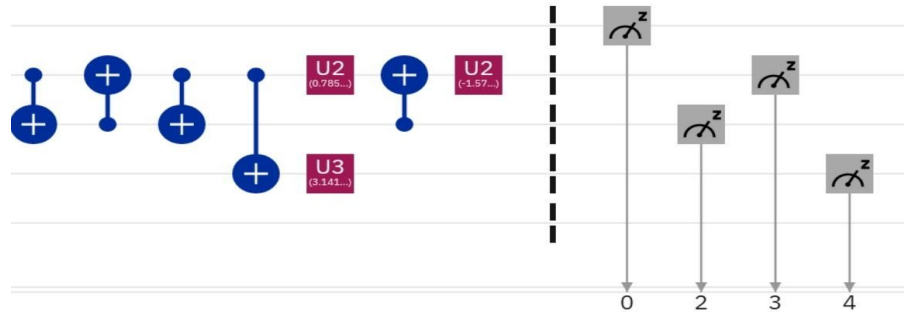

figure 10. Portion of the transpiled circuit corresponding to figure 7. (diagram continues to the left). Measurements were done at the end of each run of the experiment, but measurements on q[0] were done first (followed by q[2], q[3], q[4]); however, the exact time for measurements was not determined.

One important aspect of the experimental setups in fig. 6,7, was that $|E2>$ was formed AFTER the state $(1/\sqrt{2})(|0>_0 +e^{i\phi} |1>_0$ was created, WITHOUT further operations on q[0]; furthermore, q[0] could be measured BEFORE the information from q[4] and q[3] became incorporated with the information from q[0] to form $|E2>$. As may be noticed in fig. 6,7, the measuring devices were placed strategically on the circuit to attempt to measure the outcome of q[0] first; according to the transpiled circuit (Fig. 9 and 10) , all measurements were done at the end, where q[0] was measured first, and qubits c[0],c[1],c[2],c[3],c[4] were the respective outputs, in that order, for the measurements on qubits q[0],q[1],q[2],q[3],q[4].

First, Notice that two operations, from a time $t_{initial}$ to a time t_{final} , were necessary to create the state $Sq[0] = \frac{1}{\sqrt{2}}$ $(|0>_0 +e^{i\phi}|1>_0$ i.e a Control Hadamard and U1(ϕ) gates were applied on q[0], which was initially in state $|0>_0$; this can be written symbolically

$$O_{Sq[0]} (q[0]; t^{initial}_{q[0]} , t^{final}_{q[0]}) \rightarrow \frac{1}{\sqrt{2}} (|0>_0 +e^{i\phi} |1>_0 ,$$

where the range $(t^{[0]}_{initial} , t^{[0]}_{final})$ is the time needed to construct the state Sq[0]. Also, in the lower part of the circuit,

$$O_{Sq[3]}(q[3]; t^{initial}_{q[3]} , t^{final}_{q[3]}) \rightarrow \frac{1}{\sqrt{2}} (|0>_3 +e^{i\phi} |1>_3 ,$$

using the same type of gates. Similarly, the operation that creates $|E2>$ can be written,

$$O_{E2} (q[0],q[1],q[2],q[3],q[4]; t^{initial}_{q[0],q[1],q[2],q[3].q[4]} , t^{final}_{q[0],q[1],q[2],q[3].q[4]}) \rightarrow |E2>.$$

Now, let's define the time $\Delta t^{\text{initial}}_{q[0]}$ required from the finalized Sq[0] to the time when it became entangled with the other qubits with the expression,

$$t^{\text{final}}_{q[0]} + \Delta t^{\text{initial}}_{q[0]} \geq t^{\text{initial}}_{q[0],q[1,\ q[2],q[3],q[4]}.$$

In this way, notice that the range ($t^{[0]}_{\text{initial}}$, $t^{[0]}_{\text{final}} + \Delta t^{\text{initial}}_{q[0]}$) overlapped with the range ($t^{[0],[2],[3],[4]}_{\text{initial}}$, $t^{[0],[2],[3],[4]}_{\text{Final}}$) because the output of $O_{Sq[0]}$, after $t^{[0]}_{\text{final}}$, was necessarily part of the input for O_{E2} to create |E2> as shown in the circuit i.e there is a CNOT gate extending from q[0] into q[4] as well as another CNOT gate connecting q[3] with q[4]]. Now, if measurements on all qubits happened at times $T_{q[0]}$, $T_{q[3]}$, $T_{q[4}$, and each measurement required time Δt^{reach} BEFORE being measured, then

$$T_{q[0]} = \Delta t^{\text{reach}}_{q[0]} + t_{q[0]}$$

$$T_{q[3]} = \Delta t^{\text{reach}}_{q[3]} + t_{q[3]}$$

$$T_{q[4]} = \Delta t^{\text{reach}}_{q[4]} + t_{q[4]}$$

where $t_{q[0]}$, $t_{q[3]}$, $t_{q[4]}$ are the times when |E2> was formed by some joint wave function dependent on $t_{q[0]}$, $t_{q[3]}$, $t_{q[4]}$; the variables $\Delta t^{\text{reach}}_{q[0]}$, $\Delta t^{\text{reach}}_{q[3]}$, $\Delta t^{\text{reach}}_{q[4]}$, were the respective times needed to obtain the results at the measuring devices after the qubits were entangled; the differences in $t_{q[0]}$, $t_{q[3]}$, $t_{q[4]}$, when the joint wave function did not vanish, were within the range of the formation of the entanglement

i.e.

$$0< |t_{q[4]} - t_{q[0]}| < \Delta t^{\text{evolution}},$$

$$0< |t_{q[3]} - t_{q[0]}| < \Delta t^{\text{evolution}},$$

$$\text{where}\quad \Delta t_{\text{evolution}} = t^{\text{final}}_{q[0]\ q[2]\ q[3]\ q[4]} - t^{\text{initial}}_{q[0]\ q[2]\ q[3]\ q[4]}.$$

The circuit was arranged so that measurements on q[0] happened first as shown in fig 6 and 7; assuming a small error $\delta t_{q[0]}$, $\delta t_{q[3]}$, $\delta t_{q[4]}$ such that $(\delta t_{q[0]} / T_{q[0]}) \approx (\delta t_{q[3]} / T_{q[3]}) \approx (\delta t_{q[4]} / T_{q[4]}) \approx 0$, implies

$$T_{q[4]} \pm \delta t_{q[4]} > T_{q[0]} \pm \delta t_{q[0]},$$

$$T_{q[3]} \pm \delta t_{q[3]} > T_{q[0]} \pm \delta t_{q[0]}$$

but the differences $(T_{q[4]} \pm \delta t_{q[4]]}) - (T_{q[0]} \pm \delta t_{q[0]})$ and $(T_{q[3]} \pm \delta t_{q[3]}) - (T_{q[0]} \pm \delta t_{q[0]})$ were not measured.
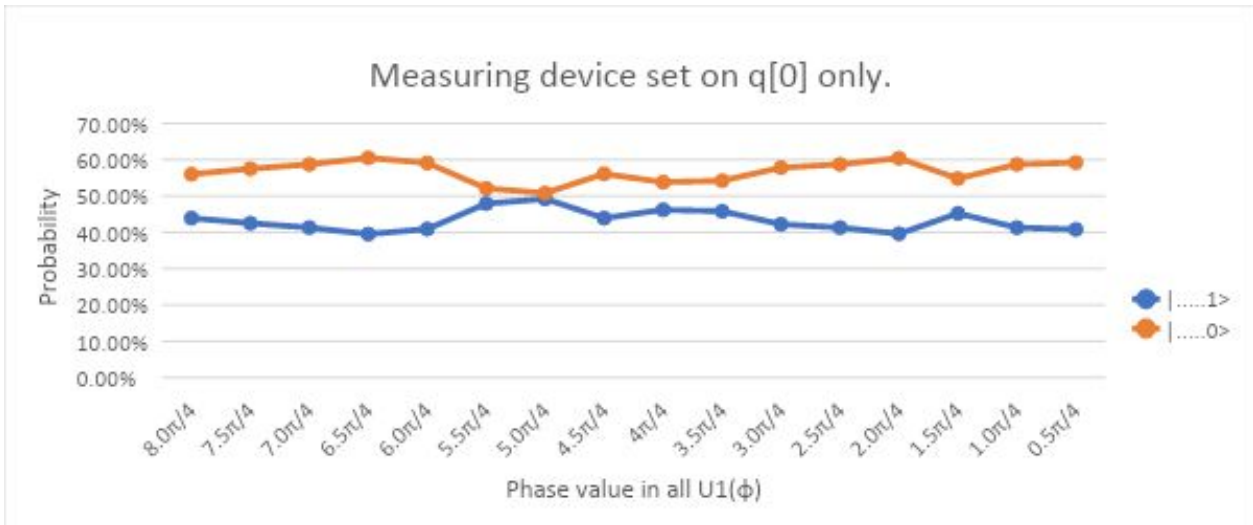
RESULTS

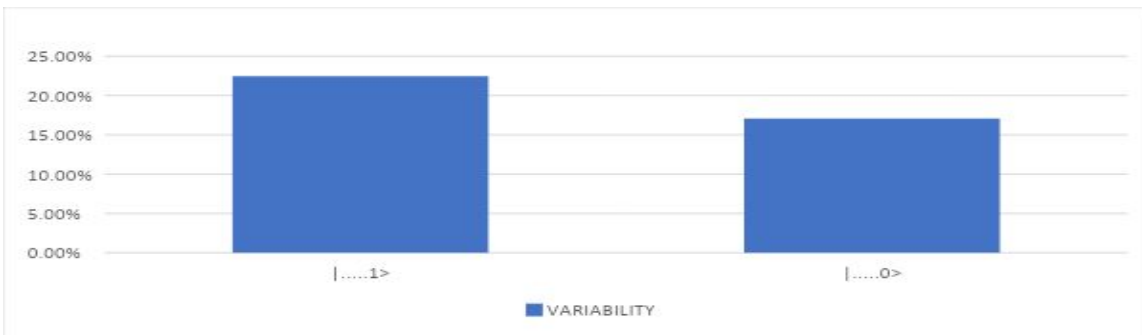**Figure 11(A).** Results from setup shown in figure 5.

Figure 11(B). Variability for data shown on figure 11(A);

Variability=(Maximum probability - Minimum probability)/Average probability.
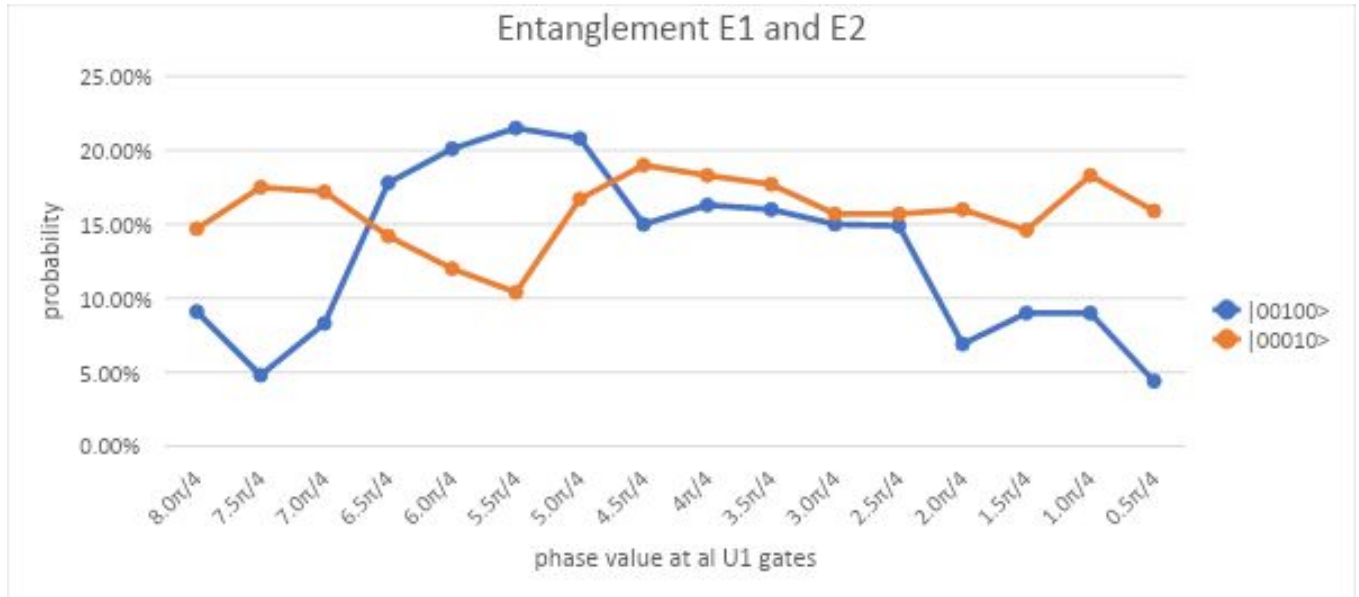
Figure 12(A). Results for the setup shown on figure 6. Orange curve corresponds to |E1> and blue line corresponds to |E2>
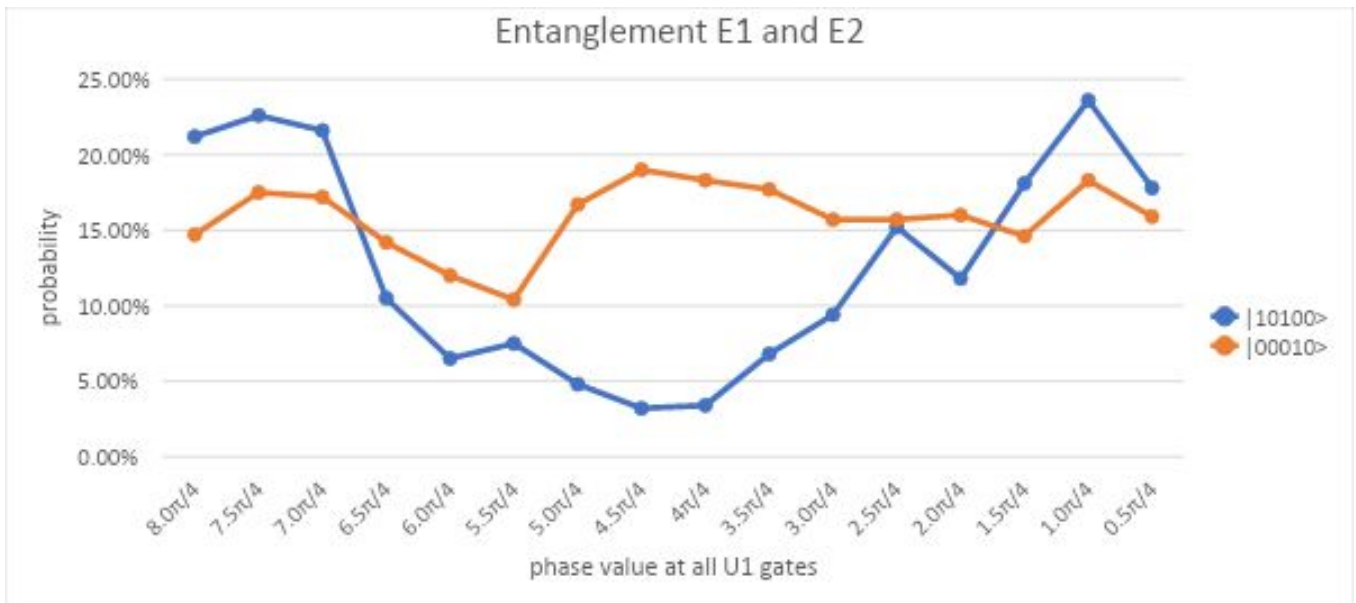

Figure 12(B). Results for the setup shown on figure 6. Orange curve corresponds to |E1> and blue line corresponds to |E2>

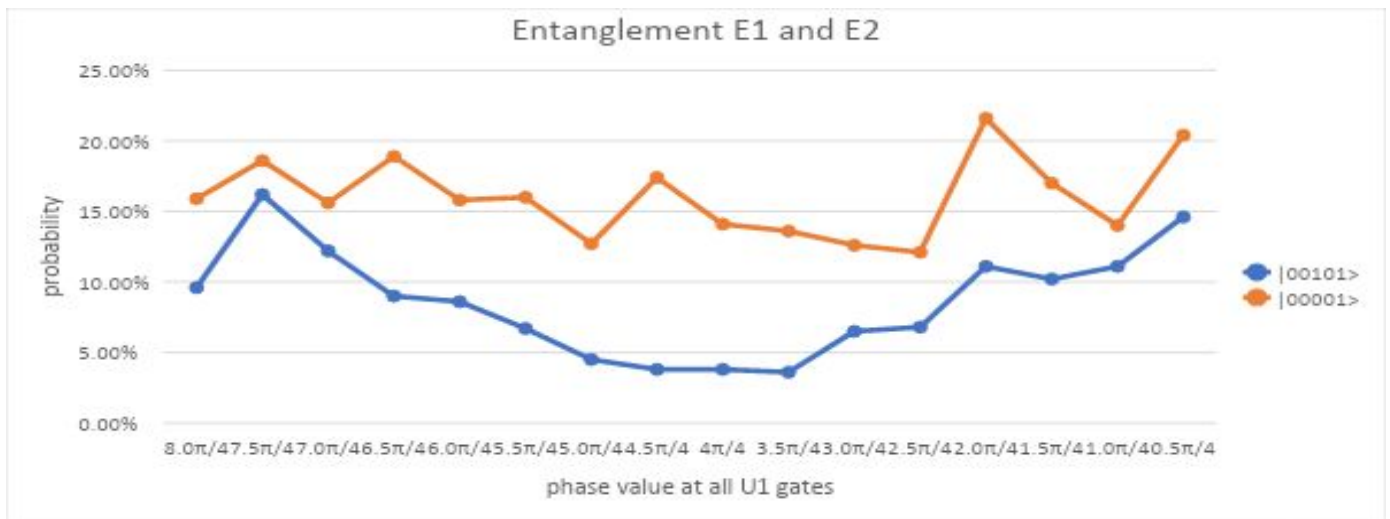**Figure 12(C).** Results for the setup shown on figure 6. Orange curve corresponds to |E1> and blue line corresponds to |E2>
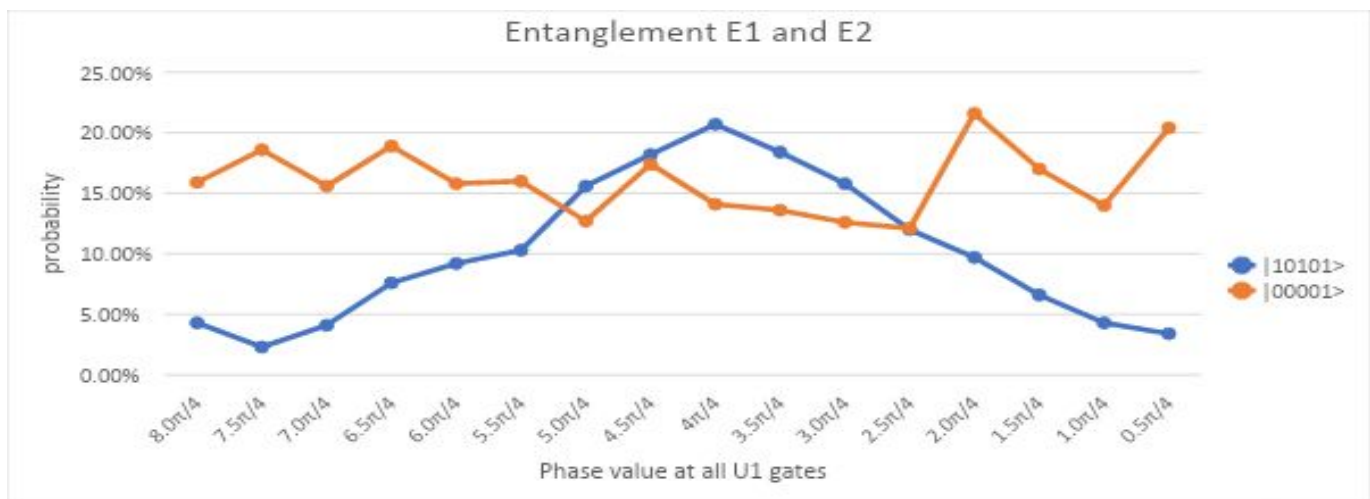
Figure 12(D). Results for the setup shown on figure 6. Orange curve corresponds to |E1> and blue line corresponds to |E2>

Figure 12(E). Variability calculations corresponding to results presented in fig. 12(A), (B), (C), (D). Variability= (Maximum Probability - Minimum Probability)/ Average probability. Variability calculations are presented as (%)
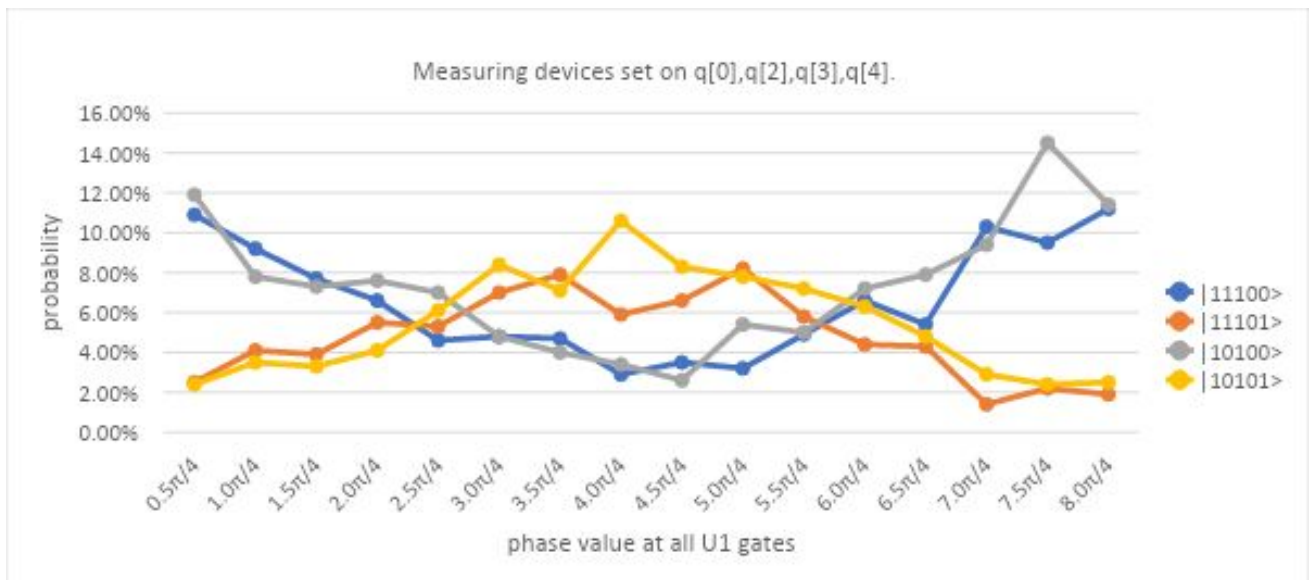
Figure 13(A). Results for the setup shown on figure 7.
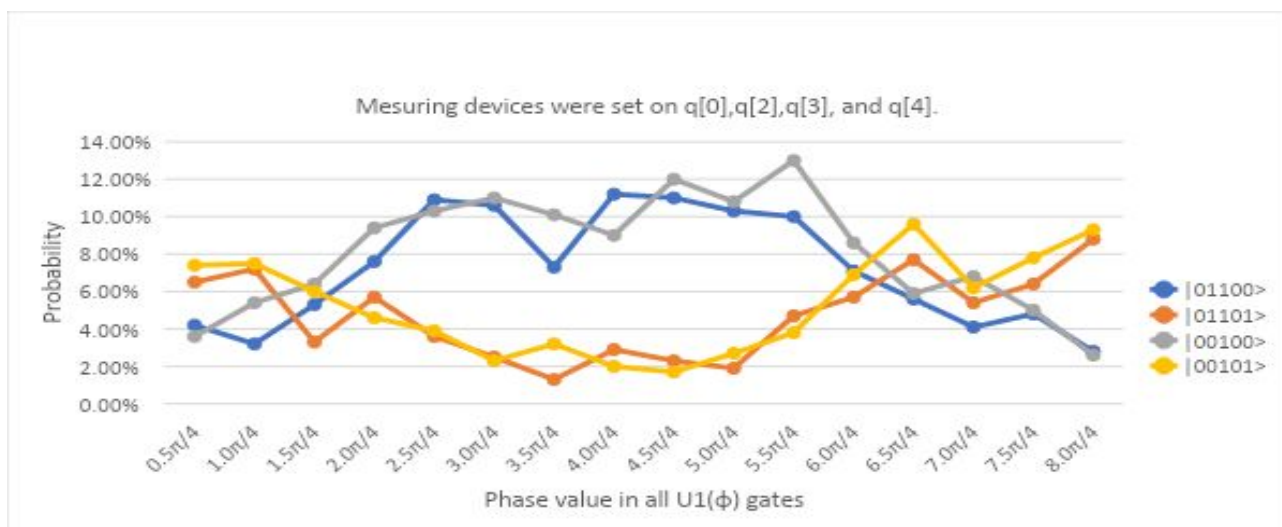
Figure 13(B). Results for the setup shown on figure 7.
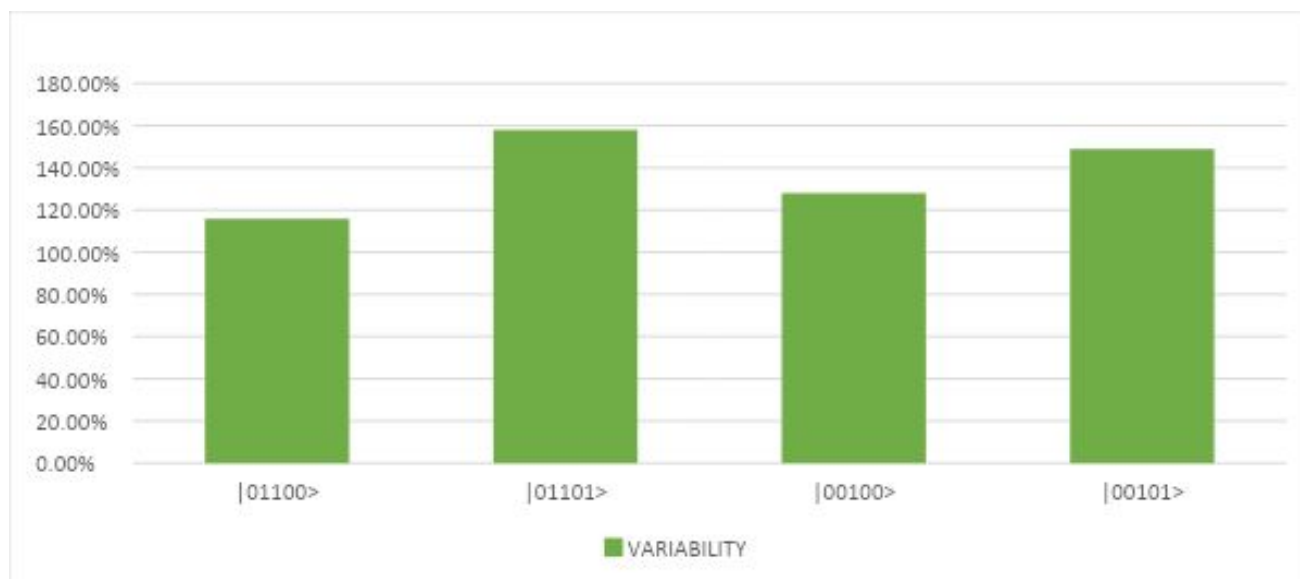
Figure 13(C). Variability calculations corresponding to results presented in fig. 13(B). Variability= (Maximum Probability - Minimum Probability)/ Average probability. Variability calculations are presented as (%)
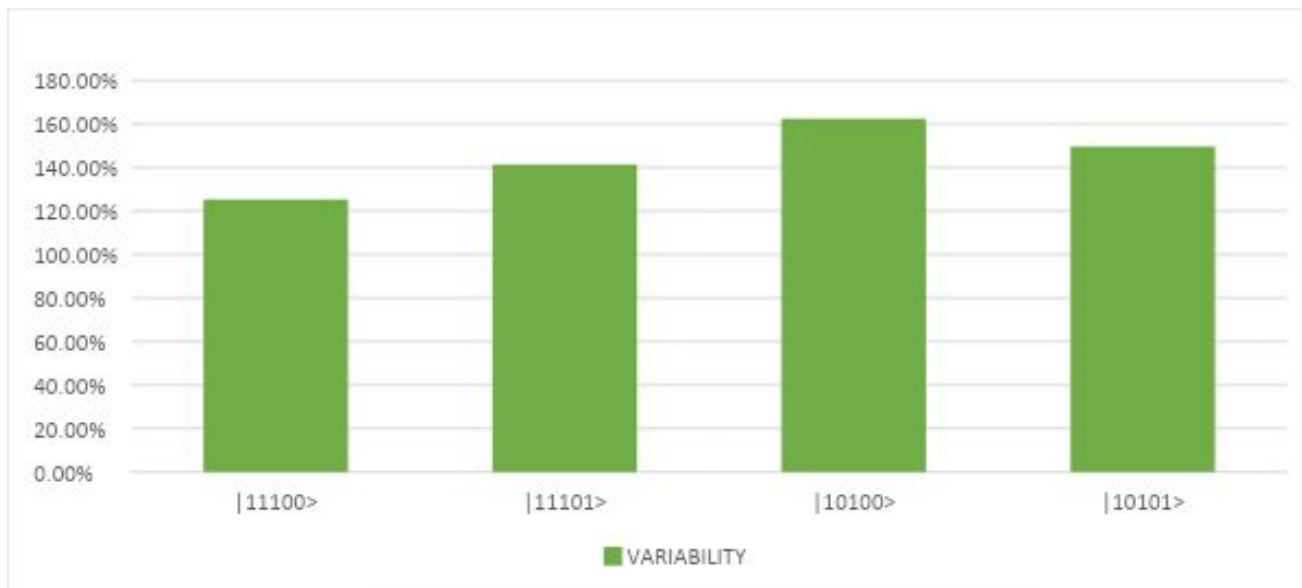
Figure 13(D). Variability calculations corresponding to results presented in fig. 13(A). Variability= (Maximum Probability - Minimum Probability)/ Average probability. Variability calculations are presented as (%)

Figure 14(A). Results for the set up shown on figure 8; Only results for |E2> are presented; however, no interference pattern, as in 12(A) and (B), was detected without q[0] measurements.
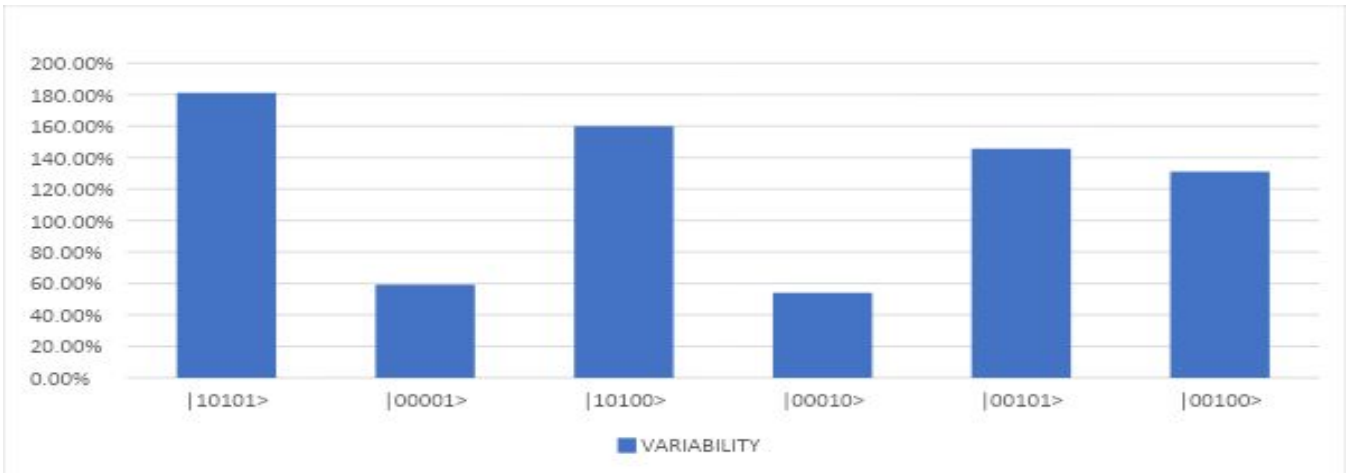
Figure 14(B). Variability calculations corresponding to results presented in fig. 14(A). Variability= (Maximum Probability - Minimum Probability)/ Average probability. Variability calculations are presented as (%).

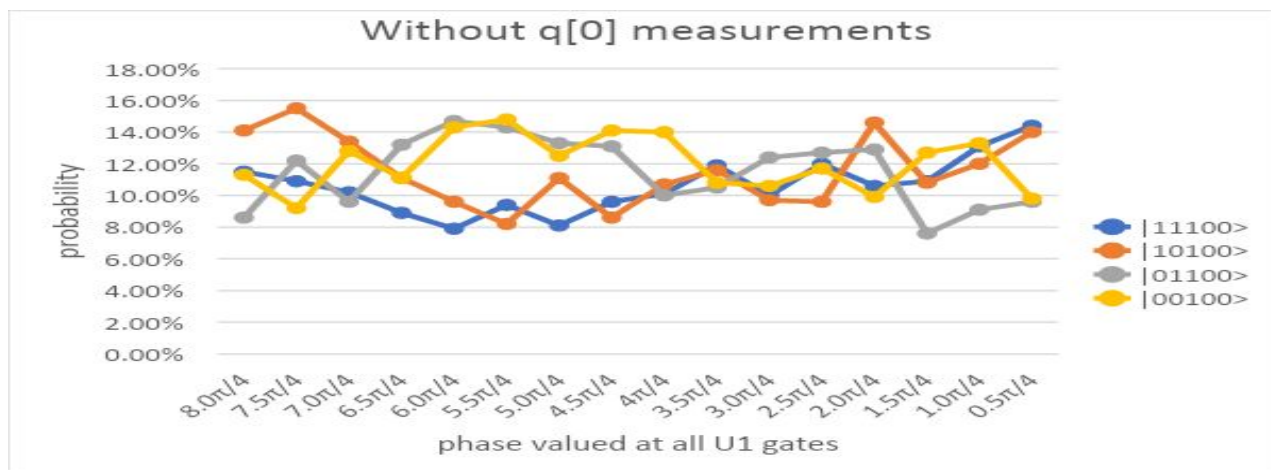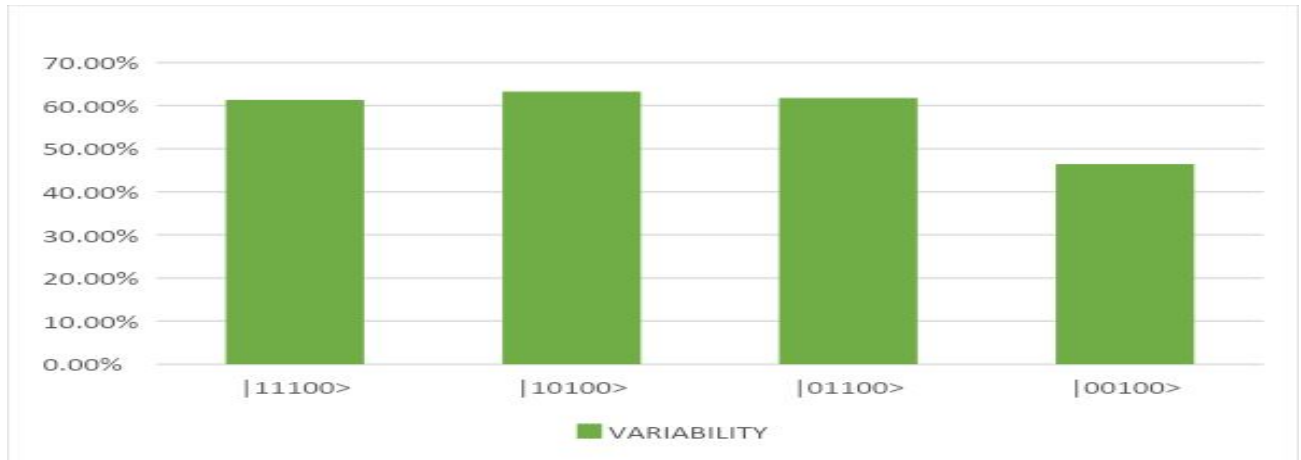Figure 11(A) presents measurements with q[0] only. The graph empirically confirms that no interference pattern can be detected by multiple measurements with q[0] even when there is a U1(ϕ) gate acting on q[0], which was expected by theory; on the other hand, the variability was not zero as shown in fig 11(B).

Figure 12(A),(B),(C),(D) presents the probability for the basis elements Ẽ1={|00010>, |00001>} and Ẽ2={|10100>, |10101>, |00100>, 00101>}, for the set up presented in figure 7, with their probabilities for different ϕ values set in all U1(ϕ) gates. (where every space in the state corresponds to the qubit measurements i.e. |c[4], c[3], c[2], c[1], c[0]> given that the measurements for each qubit q[0], q[1], q[2], q[3], q[4] was delivered on qubits c[0],c[1],c[2],c[3],c[4] respectively; note that the order in the state factors is opposite to the order that was presented in the methods section). Some of the numbers obtained in the computational basis were "0" when no measurements were done on those qubits just like when an actual measurement on the those qubits corresponded to |0>; thus, measurement on q[2] allowed to interpret the results and make the distinction i.e when the corresponding space for q[2] in the computational basis was "0", only the the spaces corresponding to q[0] and q[1] were measured (that is, the last two digits in the element of the basis output) e.g. when the space for q[2] was "1", then q[0] and q[4] were in fact measured (the first and last digit in the basis) as opposed to just be marked "0" because no measurement was done (all qubits started in state |0>, if no measurement was done, the state remains at zero; however, in the results presented, the "0" for q[3], in fig 12(A)-(D), meant that no measurement was done on that qubit). In this way, the sets Ẽ1 and Ẽ2, indicated in the graphs, corresponded to entanglements |E1> and |E2> respectively. Inspection of the two graphs allowed to determine that the probability for {|10100>, |00101>}, a function of ϕ, had the shape of a $\propto \cos^2(\phi/2)$ like function. In the same way, the graphs for {|00001>,|00010>} are presented and contrasted with Ẽ2. Notice that the shape for the probability of {|10101>, |00100>} , as a function of ϕ, has a $\propto \sin^2(\phi/2)$ shape. The bar graphs (fig. 12(E)) presents the measurements of variability; the variabilities corresponding to |00010> and |00001> were less than 1, where as the variability for both |10101> and |10100> were greater than 1.

Now, when a measuring device was set on q[0], together with measuring devices on q[2], q[3], q[4], eight interference patterns were obtained (fig 13(A),(B)). Each of the basis elements {|01100>, |01101>, |00100>, |00101>, |11100>, |11101>, 10100>, |10101>} corresponded to the eight terms in expression (20). Notice that for each graph, there were two sets of overlapping curves, being either concave up or down, while the minimum and maximum occurred in the middle of the range; the equality suggested by the overlapping of the curves refers to equalities (37); the results were consistent with figures 12(A)-(D) because the the overlapping curves corresponded to the same value for q[0] (both of the states corresponding to the overlapping curves in fig. 13(A),(B) had the same digit at the end); in this way, the results supported also relations (36) given that the outcome of q[3] did not make a difference when measuring the probability as a function ϕ.

In this way, one interesting aspect of the experimental setup was that, when measuring only q[1], q[3], q[4] (and q[2]), no interference pattern was observed by changing the phase value on all U1 gates. The results are presented in fig. 14(A); Variability was less than 1 (fig. 14(B)). It may be easily observed that the interference pattern disappeared once q[0] was not measured with the other qubits in entanglement |E2> (given that "1" was the output for q[2] in all the basis elements) as was observed in fig. 13(A) and (B). In this way, the "eraser" part of the circuit, corresponding to the gates on q[3] and q[4], did not result in an interference pattern when measurements on those qubits were done without measurement with q[0].

DISCUSSION

Results show that it is possible to differentiate between entanglements |E1> and |E2>; the former gives a lower variability in the elements of its computational basis than the latter (fig. 12(E)). Furthermore, the patterns observed in the computational basis corresponding to |E2>, as a function of the phase value ϕ, when the measuring devices were at q[0], q[3], q[4], (and q[2]) do resemble $\propto \cos^2(\phi/2)$ and $\propto \sin^2(\phi/2)$ functions, as were expected by theory i.e. the graphs were concave up or down as expected by theory (fig. 13(A)-(B)), absolute maximum and minimum values occurred within $\pi \pm (\pi/4)\,rad$, the plotted lines on figures 13(A)-(B) crossed one another at $(\pi/2)\pm(\pi/4)$ and $(3\pi/2)\pm(\pi/4)$; in contrast, these characteristics, typical of an interference pattern with waves, did not happen neither the times when|E1> was activated nor when measurements of q[0] were done without the other qubit.

Results confirmed that the interference pattern was the result of the joint measurements of q[0] with q[4] (and q[3] and q[2], but q[4] was necessary to attain an interference pattern whereas q[3] and q[2] merely helped to obtain clearer results), as shown in fig. 12(A)-(B), not the result of measurements on q[4] (with q[3] and q[2]) alone, as shown in fig. 14(A), when |E2> happened; The joint multiple histories could be attributed to any of the qubits, when |E2> happened, in which the interference pattern could be associated with one of the qubits as long as the others were measured as well and considered detector qubits; that is, one of the qubits can be considered to be the one observed and the other qubits can be considered the observer, a typical perspective in the relational interpretation of quantum mechanics [18]. In this paper, q[0] was regarded as the observed qubit, while the others were ancillary qubits. Although measurements on q[3] and q[4] (and q[2]) were not sufficient to detect an interference pattern alone, as shown in fig. 14(A), it was the state of q[0], before q[0] became entangled with q[3] and q[4], what allowed to interpret q[0] in the state $A_0|0>_0 + B_0(\phi)|0>_0$ or $C_0|1>_0 + D_0(\phi)|1>_0$ a time $t^{final}_{q[0]} + \Delta t^{initial}_{q[0]}$ later, once q[0] became entangled with the rest of the qubits to form |E2>. In this way, by measuring q[0] first, as shown in fig 9-10, no detectable interference pattern was measured in |E2> for a brief moment (assuming a low uncertainty in the time measurements to be able to establish a sequence of measurements), but once the other ancillary qubits were measured, an interference pattern occurred, changing the history of q[0] where the phase difference causing the interference pattern could be attributed to the state of q[0].

The probability functions presented in fig 12(A)-(D) as well as fig. 13(A) and (B), resulting from the complex coefficients corresponding to each computational basis element, can be attributed to other qubits that formed the computational basis, not only q[0], by the associative property of tensor products as presented in expression (11) e.g. Notice that the expression for |E1> can be also written

$$|E2> = |0>_0 |0>_1 |1>_2 |+>_3 (d(\phi)|1>_4)+$$

$$|1>_0 |0>_1 |1>_2 |->_3 (f(\phi)|1>_4)+$$

$$|0>_0 |0>_1 |1>_2 |->_3 (g(\phi)|0>_4)+$$

$$|1>_0 |0>_1 |1>_2 |+>_3 (h(\phi)|0>_4); \qquad (38)$$

In this interpretation, the phase differences that led to the interference patterns in the results can be attributed to the state of q[4] rather than q[0]; however, in the experimental set up, it was only q[0] that was part of two englements, |E1> and |E2>, where the outcomes were either $|0>_0$ or $|1>_0$, with equal probability to be in either entanglement; therefore, it is only in q[0] where both the "down" state ($|0>_0$) and the "up" state ($|1>_0$) could be interpreted as having been in a state that not only did not lead to an interference pattern sometimes, but also in a state that produced an interference pattern at other times, whose type of outcome (either $\propto \cos^2(\phi/2)$ or $\propto \sin^2(\phi/2)$ depended on the relevant constituent qubit measurements; moreover, q[0] was measured first to be able to "erase" the constant probability pattern that q[0] alone would present (fig. 5). Both interpretations are equally valid; the particular interpretation does not change the physical situation: if more quantum gates were applied on q[0] once it were interpreted to be in a state $A_0(\phi)|0>_0 + B_0(\phi)|0>_0$ or $C_0(\phi)|1>_0 + D_0(\phi)|1>_0$ after measurements of the other relevant qubits, the outcome of operating further on q[0], as if actually being in either $A_0(\phi)|0>_0 + B_0(\phi)|0>_0$ or $C_0(\phi)|1>_0 + D_0(\phi)|1>_0$ by means of gates on q[0], would be consistent with joint measurements of q[0] with the other qubits that formed the entanglement. In this way, in wheeler's interpretation, one may say the analogy that when multiple measurements of q[0] were done with q[1], while both were |E1>, q[0] had the probability distribution of a "particle" moving through a slit and falling on a screen, but when q[0] was in an entanglement |E2>, the state of q[0] was that of two waves that interfered; Consequently, the interpretation presented in this paper that the evolution of ($|0>_0 +e^{i\phi} |1>_0$) into { $A_0(\phi)|0>_0 + B_0(\phi)|0>_0$, $C_0(\phi)|1>_0 + D_0(\phi)|1>_0$ } after q[0] became entangled with the rest of the qubits that formed |E2> and those ancillary qubits were measured, does NOT imply that the measurements done in all the relevant qubits caused the interference pattern specifically at q[0]; that is, the evolution is one possible interpretation out of other possible ones [18]; on the other hand, given that the circuit allowed q[0] to be part of two entanglements |E1> and |E2>, where both outcomes |0> and |1> were possible, and where q[0] was measured first, it may be said that measurements with the other qubits "erased" the state of q[0], in a non-causal way [17], in relation to those detecting qubits, as it is the case in the DCQEE with their homologous detectors.

In the DCQEE, there is a parallel interpretation that can be made where the interference pattern observed when joint measurements with D_0, D_1 ,D_2 happen can be attributed arbitrarily to a phase difference occurring at any of the detectors. The interference like pattern observed when D_0 is moved in the x direction, implying a phase value change for different values of x, is not only possible to attribute to phase differences in the information arriving at D_0 from both A and B as a function $\Delta\phi_{D0}(x)$, but is also possible to attribute those phase changes to D_1 ,D_2 by transforming every point x into a phase change to the information that arrives at D1 or D2 by means of a function $\Delta\phi(x)$ given that the pairs of photons created at A and B were entangled; nevertheless, attributing the interference pattern to D_0 is obvious given that D_0 is being moved along the x direction as it is typical in a double slit experiment; instead, for a non-orthodox interpretation, the interference pattern can be attributed to D_1 ,D_2 where the time variables when the joint wave function occur, originally given by

$$t_0 = T_0 + (L_0/c),$$

$$t^{A \text{ or } B}_1 = T_1 + (L_1/c),$$

$$t^{A \text{ or } B}_2 = T_2 + (L_2/c), \qquad\qquad (39)$$

in the the expression for joint rates (1), (2), (3), have to be modified so that the times $\tau_1 = \Delta\phi_1(x)/\Omega_1$ or $\tau_2 = \Delta\phi_2(x)/\Omega_2$ can be added or subtracted to t_1 or t_2, respectively, when the information arrived to D_1 or D_2 from A or B, to make joint rate measurements as D_0 sampled points along the x direction; in this way, instead, t_2, t_3 can be written as functions of x, while t_0 remains independent of x:

$$t_0 = T_0 + (L_0/c),$$

$$\{ t^A_1(x) = T_1 + (L_1/c) + \Delta\phi^A_1(x)/\Omega_1 , \; t^B_1(x) = T_1 + (L_1/c) + \Delta\phi^B_1(x)/\Omega_1 \}$$

or

$$\{ t^A_2(x) = T_2 + (L_2/c) + \Delta\phi^A_2(x)/\Omega_2 , \; t^B_2(x) = T_2 + (L_2/c) + \Delta\phi^B_2(x)/\Omega_2 \}.$$

(40)

In this interpretation, when quantum information from A and B arrived at D_0 , there was no phase difference

$$\Delta\phi_1(x) = \{ \phi^A_1(x) - \phi^B_1(x) , \; \phi^A_1(x) + \phi^B_1(x) \}$$

or

$$\Delta\phi_2(x) = \{ \phi^A_2(x) - \phi^B_2(x) , \; -\phi^A_2(x) + \phi^B_2(x) \}, \qquad (50)$$

but there were phase differences, $\Delta\phi_1(x)$ or $\Delta\phi_2(x)$, at D_1 or D_2 ,corresponding to their joint wave function times $t^A_1(x)$, $t^B_1(x)$ or $t^A_2(x)$, $t^B_2(x)$ for the quantum information from A and B; from the above and the expressions for the joint wave functions in the DCQEE (), we can write

$$\psi(t_0, t^A_1(x)) \propto \exp(-\Omega_0 t_0 - [\Omega_1 t_1 + \phi^A_1(x)]),$$

$$\psi(t_0, t^B_1(x)) \propto \exp(-\Omega_0 t_0 - [\Omega_1 t_1 + \phi^B_1(x)]),$$

$$\psi(t_0, t^A_2(x)) \propto \exp(-\Omega_0 t_0 - [\Omega_2 t_2 + \phi^A_2(x)]),$$

$$\psi(t_0, t^B_2(x)) \propto \exp(-\Omega_0 t_0 - [\Omega_2 t_2 + \phi^B_2(x)]); \qquad (51)$$

In this way, as D_0 moved along the x direction, sampling points, the intensity of joint rate detections varied as a result of different phase differences that can be interpreted to have occurred at D_1 or D_2. Furthermore, if multiple measurements with D_0 alone had not produced an interference pattern by itself, but only when joint measurements with D_1 or D_2 are performed, the interference pattern still could be attributed to a phase difference at D_1 or D_2; of course, even in the such a case that D_0 were not sufficient to obtain phase difference, it would still be possible to interpret the phase difference to occur at D_0 if joint measurement with D_1 or D_2 were done given that the phase difference can be associated, mathematically speaking, with any of the terms in the exponential. That is, from the expressions for $\psi(t_0, t^A_1(x))$, $\psi(t_0, t^B_1(x))$, $\psi(t_0, t^A_2(x))$, and $\psi(t_0, t^B_2(x))$ one may easily see that the phase differences , $\Delta\phi_1(x)$ or $\Delta\phi_2(x)$, can be interpreted as associated with either measurements at D_0 or with measurements at D_1 or D_2 that lead to an interference pattern for each x position, much like, in the results obtained in the present experiment, the phase difference ϕ for all U1(ϕ) gates can be interpreted to happen at either q[0] or q[4].

Notice that the expressions for the wave functions in the DCQEE can be written,

$$\psi(t_0, t^A_1(x)) \propto \psi_0(t_0) \psi_1(t^A_1)$$

$$\psi\ (t_0, t^B_1(x)) \propto [\exp (i\ \Delta\ \phi_1(x))]\ \psi_0\ (t_0)\ \psi_1\ (t^A_1)$$

$$\psi\ (t_0, t^A_2(x)) \propto\ \psi_0\ (t_0)\ \psi_2\ (t^A_2)$$

$$\psi\ (t_0, t^B_2(x)) \propto [\exp (i\ \Delta\ \phi_2(x))]\ \psi_0\ (t_0)\ \psi_2(t^A_2), \qquad (52)$$

which are analogous to the terms in $|E2\rangle$, corresponding to the basis elements shown in blue on fig 12(A)-(D) (corresponding to the terms in expression (28)), when their respective two-term complex coefficients in set (30) are multiplied by their respective basis elements, allowing to express the outcome in terms of the phase ϕ that was used to obtain the results:

$$\eta_{01}{}^A \propto\ |0\rangle_0 \ldots |+\rangle_3\ |1\rangle_4$$

$$\eta_{01}{}^B \propto [\exp (i\varphi)]|0\rangle_0 \ldots |+\rangle_3\ |1\rangle_4$$

$$\eta_{11}{}^A \propto \text{Exp}\ (i\phi)|1\rangle_0 \ldots |-\rangle_3\ |1\rangle_4$$

$$\eta_{11}{}^B \propto -[\text{Exp}\ (2i\phi)]|1\rangle_0 \ldots |-\rangle_3\ |1\rangle_4$$

$$\eta_{00}{}^A \propto\ |0\rangle_0 \ldots |-\rangle_3\ |0\rangle_4$$

$$\eta_{00}{}^B \propto -\text{Exp}\ (i\phi)|0\rangle_0 \ldots |-\rangle_3\ |0\rangle_4$$

$$\eta_{10}{}^A \propto \text{Exp}\ (i\phi)|1\rangle_0 \ldots |+\rangle_3\ |0\rangle_4$$

$$\eta_{10}{}^B \propto [\text{Exp}\ (2i\phi)]|1\rangle_0 \ldots |+\rangle_3\ |0\rangle_4; \qquad (53)$$

the coefficients for both ψ and η can be associated with any of the state-factors that form ψ and η while maintaining the other state-factors with a coefficient of 1; each state-factor has variables only for either the detectors D_i , in the ψ case, or qubits q[j] in the η case. Associating the coefficients with one type of state-factor can be interpreted as actually happening to that particular state-factor and, thus, describing the history of that state-factor when multiple measurements are implying the phase differences.

Also, just like the interference pattern in DCQEE was the result of two wave functions that depended on joint times , $\psi_A\ (t_0, t^A_2) + \psi_B\ (t_0, t^B_2)$, the interference patterns obtained in fig 12(A)-(B) (only the blue curves) and 13(A),(B), can be written as a joint superposed time dependent function

$$H_{kl} = \eta_{kl}{}^A\ (t_{q[4]}, \ldots, t_{q[0]}) + \eta_{kl}{}^B\ (t_{q[4]}, \ldots, t_{q[0]}) \qquad (54)$$

where the superscripts and subscripts identify the eight expressions in (53); the time variables in the functions are related to the times of measurements by

$$t_{q[0]} = T_{q[0]} - \Delta t^{reach}{}_{q[0]} ,$$

$$t_{q[1]} = T_{q[1]} - \Delta t^{reach}{}_{q[1]} ,$$

$$t_{q[2]} = T_{q[2]} - \Delta t^{reach}{}_{q[2]} ,$$

$$t_{q[3]} = T_{q[3]} - \Delta t^{reach}{}_{q[3]} ,$$

$$t_{q[4]} = T_{q[4]} - \Delta t^{reach}{}_{q[4]} ,$$

where $T_{q[0]}$, $T_{q[1]}$, $T_{q[2]}$, $T_{q[3]}$, $T_{q[4]}$ were the times when measurements were done, and $\Delta t^{reach}{}_{q[1]}$, $\Delta t^{reach}{}_{q[2]}$, $\Delta t^{reach}{}_{q[3]}$, $\Delta t^{reach}{}_{q[4]}$, $\Delta t^{reach}{}_{q[5]}$ were the times needed to reach the measuring detector and carry out the measurement in their respective devices after the qubits were processed by all the gates in the circuits shown in figures 5-8.

Conclusion

The output of the circuit in fig. 5, where only measurements on q[0] were done, was a constant probability pattern regardless of the phase value ϕ set in the U1(ϕ) gates on that qubit; fig. 11(A) shows the result. Also, in entanglement |E1>, the probability was independent of the phase value ϕ, but there was a an interference like pattern when the entanglement |E2> happened (Both are contrasted in fig 12(A)-(D); the circuit used to obtain results is shown on fig. 6). Because of relations (11) and (12), the interference can be attributed to any of the qubits involved in |E2>; the phase value was interpreted to have occurred in q[0] when it was jointly measured with the other qubits; the possible histories for q[0], after measuring relevant qubits, are shown in the set of expressions (35), but regarding the other qubits as detectors [18]; an analogous interpretation can be made of the DCQEE by a replacing expressions (39) with expression (40), and attributing the phase difference $\Delta\phi_1(x)$ or $\Delta\phi_2(x)$ to either D_0 or the detectors D_1, D_2 by associating the phase difference, mathematically speaking, with the terms in the exponents in expressions (51). In the present experiment, it was shown that measurements WITHOUT q[0] were not sufficient to create an interference pattern, (using the setup shown on fig 8, whose corresponding results are shown in 14(A)) but the interference appeared when q[0] was included in the measurement (fig. 13(A),(B)). Measurements on q[0] were arranged to be done first in all experimental setups intended to obtain an interference pattern (fig. 6,7); however, the uncertainty in the time measurements was not determined, but it was assumed to be small enough so that at least some of the measurements on q[0] were done before the measurements on the other qubits and |E2> "erased" the history of $|0>_0$ or $|1>_0$, whose probabilities became dependent on ϕ, after measurements with the detecting qubits, transforming $|0>_0 + e^{i\phi}|1>_0$ into one of the states in the set (35), depending on the outcome of the detecting qubits, and treating those detecting qubits as being independent of ϕ, effectively changing the history of q[0] in relation to the detecting qubits as if the future could influence the past for a brief moment.

BIBLIOGRAPHY

[1] J. A. Wheeler, "Mathematical Foundations of Quantum Mechanics,ed A.R. Marlow, Academic Press, New York, 1978, 0-48

[2] D. Bohm and B.J. Hiley, "The Undivided Universe", Routledge London and NewYork 1993.

[3] N. Bohr, Atomic Physics and Human Knowledge, Science Editions, New York, 1961, 50.

[4] The Feynman Lectures on Physics Vol. III, Feynman-Leighton-Sands, Quantum Mechanics, Sec. 1-7.

[5] Wheeler, J.A: Information, physis, quantum: The search for links. In: Zureck, W.H (ed) Complexity, Entropy and the Physics of information, Santa Fe institute Studies in the Sciences of Complexity, pp 13-14.

[6] Jacques, Vincent; Wu, E; Grosshans, Frédéric; Treussart, François; Grangier, Philippe; Aspect, Alain; Roch, Jean-François (2007). "Experimental Realization of Wheeler's Delayed-Choice Gedanken Experiment". Science. 315 (5814): 966–8. arXiv:quant-ph/0610241

[7] Manning, A. G; Khakimov, R. I; Dall, R. G; Truscott, A. G (2015). "Wheeler's delayed-choice gedanken experiment with a single atom". Nature Physics. 11 (7): 539. Bibcode:2015NatPh..11..539M. doi:10.1038/nphys3343.

[8] Marian O. Scully and Kai Druhl, Phys. Rev A **25**, 2208-Published 1 April 1982

[9] Herzog, T.J., Kwiat, P.G., Weinfurter, H., Zeilinger, A. (1995). "Complementarity and the quantum eraser"
(PDF). Physical Review Letters 75 (17): 3034–3037.

[10] Kim, Y.H, R. Yu; S.P. Kulik; Y.H. Shih; Marlan Scully   (2000). "A Delayed Choice Quantum Eraser".
Physical Review Letters 84:

[11] Walborn, S. P. et al. (2002). "Double-Slit Quantum Eraser".   Phys. Rev. A 65 (3): 033818. arXiv:quant-
ph/0106078. Bibcode:2002PhRvA..65c3818W. doi:10.1103/PhysRevA.65.033818.

[12] Ma, Xiao-Song; Kofler, Johannes; Qarry, Angie; Tetik, Nuray; Scheidl, Thomas; Ursin, Rupert; Ramelow, Sven; Herbst, Thomas; Ratschbacher, Lothar; Fedrizzi, Alessandro; Jennewein, Thomas; Zeilinger, Anton (2013). "Quantum erasure with causally disconnected choice". Proceedings of the National Academy of Sciences. 110 (4): 110–1226. arXiv:1206.6578. Bibcode:2013PNAS..110.1221M. doi:10.1073/pnas.1213201110. PMC 3557028. PMID 23288900.

[13] Peruzzo, Alberto; Shadbolt, Peter; Brunner, Nicolas; Popescu, Sandu; O'Brien, Jeremy L (2012). "A Quantum Delayed-Choice Experiment". Science. 338 (6107): 634–637.

[14] Demonstration of quantum delayed-choice experiment on a quantum computer
Pranav D. Chandarana, Angela Anna Baiju, Sumit Mukherjee, Antariksha Das, Narendra N. Hegade, Prasanta K. Panigrahi arXiv:2004.04625 [quant-ph]
or arXiv:2004.04625v2 [quant-ph] for this version)

[15] Realization of an entanglement-assisted quantum delayed-choice experiment. Tao Xin, Hang Li, Bi-Xue Wang, and Gui-Lu Long. Phys. Rev. A 92, 022126 (2015)

[16] Narasimhan, Ashok; Kafatos, Menas C (2017). "Wave particle duality, the observer and retrocausality". AIP Conference Proceedings. 1841 (1): 040004. arXiv:1608.06722.

 [17] "A Very Common Fallacy in Quantum Mechanics: Superposition, Delayed Choice, Quantum Erasers, Retrocausality, and All That" David Ellerman, arXiv preprint arXiv:1112.4522, 2011

[18] Rovelli, C.: "Relational Quantum Mechanics"; International Journal of Theoretical Physics 35; 1996: 1637-1678; arXiv:quant-ph/9609002